


TITLE: Mapping the distribution of language related genes *FoxP1*, *FoxP2* and *CntnaP2* in the brains of vocal learning bat species.

AUTHORS:

Pedro M. Rodenas-Cuadrado¹, Janine Mengede¹, Laura Baas¹, Paolo Devanna¹, Tobias A. Schmid², Michael Yartsev^{2,3}, Uwe Firzlaff⁴ and Sonja C.Vernes^{1,5,*} 

¹Neurogenetics of Vocal Communication Group, Max Planck Institute for Psycholinguistics, PO Box 310, Nijmegen, 6500 AH, The Netherlands

²Helen Wills Neuroscience Institute, UC Berkeley, 132 Barker Hall #3190, Berkeley, CA, 94720, USA.

³Department of Bioengineering, UC Berkeley, Stanley Hall, 306 University of California, Berkeley, CA 94720, USA.

⁴Department Tierwissenschaften, Lehrstuhl für Zoologie, TU München, Liesel-Beckmann-Str. 4, Freising-Weihenstephan, München, 85354, Germany

⁵Donders Centre for Cognitive Neuroimaging, Kapittelweg 29, Nijmegen, 6525 EN, The Netherlands

*Corresponding author: Sonja.Vernes@mpi.nl

This article has been accepted for publication and undergone full peer review but has not been through the copyediting, typesetting, pagination and proofreading process which may lead to differences between this version and the Version of Record. Please cite this article as an 'Accepted Article', doi: 10.1002/cne.24385

© 2018 Wiley Periodicals, Inc.

Received: Jun 12, 2017; Revised: Nov 07, 2017; Accepted: Nov 27, 2017

ABSTRACT

Genes including *FOXP2*, *FOXP1* and *CNTNAP2*, have been implicated in human speech and language phenotypes, pointing to a role in the development of normal language-related circuitry in the brain. Although speech and language are unique human phenotypes, a comparative approach is possible by addressing language-relevant traits in animal model systems. One such trait, vocal learning, represents an essential component of human spoken language, and is shared by cetaceans, pinnipeds, elephants, some birds and bats. Given their vocal learning abilities, gregarious nature, and reliance on vocalisations for social communication and navigation, bats represent an intriguing mammalian system in which to explore language-relevant genes. We used immunohistochemistry to detail the distribution of FoxP2, FoxP1 and Cntnap2 proteins, accompanied by detailed cytoarchitectural histology in the brains of two vocal learning bat species; *Phyllostomus discolor* and *Rousettus aegyptiacus*. We show widespread expression of these genes, similar to what has been previously observed in other species, including humans. A striking difference was observed in the adult *Phyllostomus discolor* bat, which showed low levels of FoxP2 expression in the cortex, contrasting with patterns found in rodents and non-human primates. We created an online, open-access database within which all data can be browsed, searched, and high resolution images viewed to single cell resolution. The data presented herein reveal regions of interest in the bat brain and provide new opportunities to address the role of these language-related genes in complex vocal-motor and vocal learning behaviours in a mammalian model system.

INTRODUCTION

How language evolved and is encoded in our biology represents one of the most challenging questions in the quest to understand what makes us human. Although language is unique to humans, we can address this topic using a comparative approach by studying language-relevant traits shared with other animals. Vocal production learning (VPL), the ability to learn to modify vocal outputs in response to auditory feedback, is a key skill employed by humans to facilitate spoken language (Janik and Slater, 2000; Petkov and Jarvis, 2012). Although VPL is a rare trait, it has been demonstrated in some birds, cetaceans, pinnipeds, elephants and some bats (Janik and Slater, 1997; Petkov and Jarvis, 2012; Knornschild, 2014). As has been shown by elegant work in songbirds, studying VPL in animal models can shed light on the neurobiological and genetic mechanisms underlying this trait (Doupe and Kuhl, 1999; Mello, 2002; Goldstein et al., 2003; Doupe et al., 2004; Jarvis, 2004; Scharff and White, 2004; Doupe et al., 2005; White et al., 2006; Haesler et al., 2007; Bolhuis et al., 2010; Hilliard et al., 2012; Petkov and Jarvis, 2012; Brainard and Doupe, 2013). To date, little is known about the neurogenetic mechanisms underlying VPL in mammalian vocal learners – partly due to difficulties performing such studies on large animals like sea mammals or elephants. However, bats are emerging as a promising mammalian system in which to address these questions given that a number of species display vocal learning abilities, their highly gregarious nature, and their amenability to lab based experiments (Knornschild, 2014; Vernes, 2017). Determining the expression patterns of genes implicated in speech and language in vocal learning bats will point to brain regions that may be important for vocal learning and allow detailed neurogenetic investigations of how these genes directly influence this complex vocal behaviour. Herein we present an in-depth histological investigation of three key genes implicated in human speech and language phenotypes (*FoxP2*, *FoxP1* and *CntnaP2*¹) in the brains of two bat species with evidence of vocal learning; *Phyllostomus discolor* (*P. discolor*) and *Rousettus aegyptiacus* (*R. aegyptiacus*).

FOXP2 was the first and is the most well characterised gene known to be involved in human language (Lai et al., 2001; Fisher and Scharff, 2009). *FOXP2* mutations were identified as a monogenic cause of speech and language disorder in an extended pedigree (known as the 'KE family') and has since been found in numerous similarly affected but unrelated individuals (Morgan A, 2016). The *FOXP1* gene is

¹Uppercase denotes the human gene, lowercase denotes mouse and mixed upper and lower is used for all other species, according to standard nomenclature. Italics are used when referring to genes and standard text is used for proteins.

closely related to *FOXP2* and mutations in this gene have also been found in children with language impairments, although unlike individuals with *FOXP2* mutations, these children often display additional deficits including autism spectrum disorder, mild to moderate intellectual disabilities and motor impairments (Hamdan et al., 2010; Lozano et al., 2015; Sollis et al., 2016). Both *FOXP2* and *FOXP1* are members of the same protein family that act to regulate the expression of other genes in the genome, determining when and where they are switched on or off (Li et al., 2004). One of the genes regulated by *FOXP2* is *CNTNAP2*, and this gene has itself been directly associated with specific language impairment in children (Vernes et al., 2008). *CNTNAP2* encodes a transmembrane protein (known as Caspr2) that facilitates clustering of proteins in specific regions of myelinated axons and at synapses (Rodenas-Cuadrado et al., 2014). Mutations in *CNTNAP2* can produce a range of phenotypes in addition to speech and language problems including autistic phenotypes, intellectual disability and epilepsy (Strauss et al., 2006; Alarcón et al., 2008; Bakkaloglu et al., 2008; Rodenas-Cuadrado et al., 2014; Rodenas-Cuadrado et al., 2016). In a vocal learning avian species (zebra finch), *FoxP2*, *FoxP1* and *CntnaP2* are all expressed in key regions of the song learning circuitry, with enrichment across different combinations of nuclei for each gene (Teramitsu, 2004; 2006; Panaitof et al., 2010; Tanimoto et al., 2010; Condro and White, 2014). These genes have also been explored in the developing human brain, and in primate and rodent models, displaying widespread expression across circuitry that contribute to vocal-motor perception and production (Ferland et al., 2003; Lai et al., 2003; Haesler et al., 2004; Teramitsu, 2004; Alarcón et al., 2008; Campbell et al., 2009; Panaitof et al., 2010; Condro and White, 2014; Gordon et al., 2016). As such, expression of these three genes is expected to be found in circuits subserving vocal-motor and/or vocal-learning pathways in bat brains.

Evidence of vocal learning has been described in bats across three different families; Phyllostomidae, Pteropodidae and Emballonuridae (Knornschild, 2014; Prat et al., 2015), and a few other bats show promise as vocal learners (Knornschild, 2014). *P. discolor* of the Phyllostomidae family was the first bat species suggested to be a vocal learner when it was shown that pups of this species modify their calls in response to the maternal calls to which they are exposed (Esser and Schmidt, 1989; Esser, 1994). *R. aegyptiacus* of the Pteropodidae family is also thought to be a vocal learner, since juveniles require vocal input from adults in order to learn the appropriate adult vocal repertoire. Features of their learned vocalizations can also be modified using auditory playback, suggestive that auditory input in this species is both necessary and sufficient for acquiring vocalizations (Prat et al., 2015). For both species the learned calls are relatively low frequency calls (in the range of ~10-60 kHz) that are laryngeally produced

and used for social communication (Esser and Schmidt, 1990; Prat et al., 2015). Both species are capable of echolocation, however the mechanisms employed are different; *P. discolor* uses frequency modulated echolocation calls generated from the larynx to navigate (Esser and Kiefer, 1996), while *R. aegyptiacus* is not capable of laryngeal echolocation, but uses tongue clicking to facilitate sonar navigation (Yovel et al., 2011). In addition to the evidence for vocal learning, *P. discolor* and *R. aegyptiacus* display a number of other advantages recommending them for study; unlike many bat species, *P. discolor* and *R. aegyptiacus* can be maintained in captive breeding colonies facilitating controlled study of the neurogenetic bases of traits like vocal learning. Furthermore, these two bat species are positioned at either end of the chiropteran phylogenetic tree (Teeling et al., 2005) making comparative study of these species likely to reveal generalizable features of vocal learning.

Herein, we report detailed expression patterns for the FoxP2, FoxP1 and Cntna2 (Caspr2) proteins, accompanied by cytoarchitectural histology, throughout the brains of *P. discolor* and *R. aegyptiacus* bats. All high-resolution images have been made available via a searchable database, providing an open access histological and neurogenetic resource. Our data reveals distributed expression of these key language-related genes and highlights brain regions where these genes may contribute to vocal communication and vocal learning in bats.

MATERIALS AND METHODS

Animal housing and conditions

P. discolor bats originated from a breeding colony in the Department Biology II of the Ludwig-Maximilians-University in Munich. In this colony animals were kept under semi-natural conditions (12 hour day/12 hour night cycle, 65 to 70 % relative humidity, 28 °C) with free access to food and water. Approval to keep and breed the bats was issued by the Munich district veterinary office. Under German Law on Animal Protection a special ethical approval is not needed for this procedure, but the number of sacrificed animals was reported to the district veterinary office.

Egyptian fruit bats (*R. aegyptiacus*) originated from a breeding colony at UC Berkeley, Berkeley, CA. The specimens used in this study were imported from a breeding facility at the Weizmann institute in Israel or captured from a natural roost near Herzliya, Israel and imported to UC Berkeley. In this colony animals were kept under semi-natural conditions (12 hour day/12 hour night reverse daylight cycle,

humidity 30-70% and temperature ranging between 70-75° F). Bats had free access to food and water. All experimental and breeding procedures were approved by the UC Berkeley Institutional care and use committee (IACUC).

Sample collection

For both species, adult bats were housed in small groups in large cages and the juvenile *P. discolor* animal was caged separately with free access to food and water prior to sample collection. *P. discolor* were euthanised by an intraperitoneally applied lethal dose of pentobarbital (0.16 mg/g bodyweight). Brains were extracted and incubated in 4% formaldehyde solution (10% Formalin) for 48 hours. *R. aegyptiacus* were euthanised via an IP injection of 0.5ml Beuthanasia-D solution (390 mg/ml sodium pentobarbital). Animals were then perfused with 200 ml of 0.025M PBS + heparin (pH 7.4) followed by 200 ml of freshly prepared 4% paraformaldehyde in 0.025M PBS (pH 7.4) delivered via a peristaltic pump. Subsequently, the brains were removed and stored in fixative (4% formaldehyde solution) for 48 hours. An adult male mouse was culled by cervical dislocation. The brain was extracted stored in fixative (4% formaldehyde solution) for ~48 hours. Experimental procedures were approved by the Animal Ethics Committee of the Radboud University Nijmegen (Nijmegen, the Netherlands) and conducted in accordance with the Dutch legislation.

Immunohistochemistry (IHC)

To generate a comprehensive view of the *P. discolor* and *R. aegyptiacus* brain, we generated serial sections of 4 µm thick tissue slices, with 49 and 45 slices per brain, respectively. Two adult males (> 1 year old) and one juvenile male (~2.5 months old) *P. discolor* animals, and one adult male (> 1 year old) *R. aegyptiacus* animal were used to generate the images included in the online atlas. Further animals were used to confirm staining pattern. Nissl staining was used to show the structural features at each depth (see Figure 1 for *P. discolor* and Figure 2 for *R. aegyptiacus*). Adjacent slides were used in IHC (described below) to determine the expression pattern of FoxP2, FoxP1 and CntnaP2.

For IHC, brains were dissected into four parts (coronally), paraffin embedded and sliced into 4µm thick sections and transferred to Superfrost plus glass slides (Menzel Gläser). The slides were dried overnight at room temperature and incubated at 57°C for 1 hour. For staining, the slides were washed in xylene for 10min and re-hydrated sequentially in 100%, 95%, 70% and 50% ethanol and water for 2min/wash. Antigen retrieval was performed as indicated in Table 1 - in either pH6 citrate buffer (Immunologic) or

pH9 Tris-EDTA buffer (Immunologic) in a microwave for 3-5min at 850W and 10min at 180W.

Endogenous peroxidase was blocked for 30min using 0.3 % H₂O₂ (Sigma) diluted in water, followed by a brief wash in water. The tissue was then encircled with a PAP pen and blocked with 10% normal serum (Vector labs) for 1 hour at room temperature. After blocking, slides were incubated overnight at 4°C with primary antibody diluted in appropriate blocking solution (see Table 1). The following day, sections were washed three times with PBS and incubated with the corresponding secondary antibody for 1 hour at room temperature. All slides, except those used with the anti-Foxp2 antibody, were then processed for ABC-DAB staining. This involved incubation with avidin-biotin-horseradish peroxidase complex (ABC) using the Vectastain kit (Vector Laboratories). Briefly, reagent A and reagent B were diluted together 1:100 in PBS and incubated for 30min at room temperature prior to addition to the tissue sections. Tissue sections were then incubated the ABC solution for 45min at room temperature and washed three times in PBS. Experiments using anti-Foxp2 antibody did not need this step as the secondary antibody Poly-HRP-GAM/R/R (Immunologic) was already conjugated to horseradish peroxidase. Sections were then incubated for 7min with diaminobenzidine (DAB) solution (Immunologic). Following colour development the slides were briefly washed in water and counterstained with Haematoxylin modified (Harris and Gill II) (Sigma) for 1 min. The slides were then washed in water, 50%, 70%, 95%, and twice in 100% ethanol 2 min each wash. Finally, the slides were washed twice in Xylene (Sigma) and coverslipped using DPX (Sigma). An overview of all antibodies and conditions used can be found in Table 1.

Antibody characterization

Primary antibodies were raised against human protein epitopes that were largely conserved with the relevant *P. discolor* and *R. aegyptiacus* proteins. Details of the antibody conditions are given in Table 1 and full details of the antibodies and characterisation are below. Secondary antibody only controls were performed for all conditions and can be found in the online database (see <https://hdl.handle.net/1839/84340C26-78EC-41BD-893B-12DE911BDA70@view>).

FOXP2-Banham mouse monoclonal antibody, clone 73A/8, was raised against N-terminal epitope corresponding to amino acids 1-86 of the human protein, (this antibody was a generous gift of Alison Banham, but is also commercially available from Millipore Cat# MABE415; RRID: AB_2721039). The antiserum stains a single band of ~80 kDa on Western blot (manufacturers' technical information). Staining with this antibody gave broadly the same staining pattern of immunoreactivity and mRNA

expression pattern that has been described previously (Ferland et al., 2003; Lai et al., 2003), apart from the exceptions noted in the results below (e.g. reduced cortical staining in *P. discolor*). No staining was seen when the antibody was used to stain brain tissue from a Foxp2 knockout mouse (see <https://hdl.handle.net/1839/8C1733D7-DA9A-4776-AEC6-0612CB7B0655@view>).

Two antibodies were used for FoxP1 detection. The FOXP1 mouse monoclonal antibody, clone UMAB89 (Origene Cat# UM800020, RRID: AB_2629133), was raised against the full length recombinant human FOXP1 protein (NP_116071). The antiserum stains a single band of ~75 kDa molecular weight on Western blot (manufacturers' technical information). The FOXP1 rabbit monoclonal clone EPR4113 (AbCam Cat # AB134055, RRID: AB_2632402) was raised against an epitope available upon request from the company. The antiserum stains a single band of ~75 kDa molecular weight on a Western blot (see <https://hdl.handle.net/1839/70A28CEC-9FA6-4058-B810-33B411090220@view>). Staining with both these FOXP1 antibodies gave the same staining pattern of immunoreactivity and mRNA expression pattern that has been described previously (Ferland et al., 2003).

CNTNAP2 (CASPR2) mouse monoclonal antibody, clone S67-25 (Novus Biological Cat #NBP1-49575, RRID: AB_10011672), was raised against a fusion protein corresponding to amino acids 96-1265 of human CASPR2. The antiserum stains a single band of ~180 kDa molecular weight on Western blot (manufacturers' technical information). Staining with this antibody gave the same staining pattern of immunoreactivity and mRNA expression pattern that has been described previously (Bakkaloglu et al., 2008; Gordon et al., 2016).

TLE4 rabbit polyclonal antibody (Origene Cat #TA330275, RRID: AB_2721043) was raised against synthetic peptide directed towards the N-terminal of human protein corresponding to amino acids 215-264. The antiserum stains a single band of ~84 kDa and a second band at ~30 kDa molecular weight on Western blot (manufacturers technical information). TLE4 was used as a layer marker for cortical layer 6 and staining with this antibody gave the same layer 6 specific staining pattern of immunoreactivity that has been described previously (Hevner, 2007; Nakagawa et al., 2017).

ROR β mouse monoclonal antibody, clone OTI1G1 (Origene Cat#TA806996, RRID: AB_2721044), was raised against a human recombinant ROR β protein fragment corresponding to amino acids 1-260. The antiserum stains a single band of ~52 kDa molecular weight on Western blot (manufacturers' technical

information). ROR β was used as a layer marker for cortical layer 4 and staining with this antibody gave the same layer 4 specific staining pattern of immunoreactivity that has been described previously (Hevner, 2007; Moroni et al., 2009; Jabaudon et al., 2012).

Expression analysis and region identification

To make a comprehensive record of expression, 12 representative sections at different tissue depths across the brain were analyzed in detail (indicated by asterisks in Figure 1 and Figure 2). For each brain region, the expression was graded for staining intensity (absent to high: - to +++) and abundance of positive cells in a region ('Rare' to 'Abundant'). Scoring was made across the cerebral cortex, striatum, thalamus, hypothalamus, midbrain, hindbrain and cerebellum. To aid in analysis of the *R. aegyptiacus* brain structures, two anatomical brain atlases were mainly used, Schneider R: Das Gehirn von *R. aegyptiacus* (Schneider, 1966) and an unpublished atlas shared by Yartsev, M. (personal communication, prepared in the laboratory of Nachum Ulanovsky at the Weizmann institute, Israel). There are no published atlases for *P. discolor*, so for this species we used the brain atlas of the closely related species *Carollia perspicillata* for analysis (Scalia, 2013). For identification of different subfields of the auditory cortex of *P. discolor* we used data published in Hoffmann et al., 2008. (Hoffmann et al., 2008). Where these atlases were incomplete or ambiguous, additional resources were used including the Allen mouse brain atlas (Lein et al., 2007), and the *Rosettus amplexicaudatus brachyotis* (Baron et al., 1996) brain atlas. Complete analysis of staining can be found in Table 2 (*P. discolor*) and Table 3 (*R. aegyptiacus*). Depths of images represented in manuscript figures are indicated in Figure 3.

Image preparation and tagging

Slides were scanned using either a Sakura VisionTek Live Digital Microscope scanner or Axio2 Zeiss microscope to a resolution of 0.55 $\mu\text{m}/\text{pixel}$ and 0.45 $\mu\text{m}/\text{pixel}$, respectively. Images were globally white balanced equally among all sections that were stained with the same antibody to match the histological slides using Photoshop CS6. Images were then meta-tagged for; species, age, experimental conditions (primary antibody, antibody concentration, antigen retrieval pH, IHC method), slicing plane and the main brain regions, e.g. cortex, striatum, thalamus.

RESULTS

We found expression of FoxP2, FoxP1 and CntnaP2 in the brains of both bat species throughout multiple regions. Expression patterns were highly conserved across the two vocal learning bat species, with a few key exceptions, which are discussed region by region, below. A summary of the expression patterns found in *P. discolor* can be found in Table 2, and *R. aegyptiacus* in Table 3.

Cerebral cortex

FoxP2, FoxP1 and CntnaP2 were all expressed in the cerebral cortex of both species, with differing layer specific expression patterns (Figures 4-5). FoxP1 and CntnaP2 did not show species-specific differences in distribution across the six layers of the cortex, however FoxP2 displayed dramatic differences between *P. discolor* and *R. aegyptiacus*.

R. aegyptiacus displayed strong and abundant expression of FoxP2 in layer 6 and deep layer 5 neurons (Figure 5a-c), consistent with the pattern found in the adult rodent cortex (See Figure 6). Strong and abundant staining was also found in layer 4 neurons in some regions of the *R. aegyptiacus* cortex along with sparse but intense staining of occasional neurons in layers 2-3. Strikingly, in adult *P. discolor* bats, FoxP2 expression was not enriched in layer 6. Instead, FoxP2 could only be identified in rare neurons spread across layers 2-6 of the cortex (Figure 4a-c). In both species, the FoxP2 protein was strongly detected in other brain regions in comparable patterns, and protein detection was confirmed via western blot (see <https://hdl.handle.net/1839/BF738ABE-E1C2-4B90-9752-47A1EF671B21@view>), showing that this difference was unlikely to be due to antibody/epitope recognition differences across the species. Given these differences, we compared layer specific markers between mouse and *P. discolor* brains. These classical markers of layer 4 and layer 6 (RorB and TLE4, respectively) indicated conservation of the broad cortical layering between mouse and *P. discolor* (Figure 6) suggesting that the FoxP2 expression differences observed in *P. discolor* did not reflect major differences in the development of cortical layering. As both *P. discolor* brains tested were male, we also compared staining in two female brains, but observed the same pattern of cortical expression (data not shown).

To determine if the expression pattern observed in *P. discolor* was consistent throughout development or a feature of adult animals, we compared expression of FoxP2 in juvenile (~2.5 months old) and adult brains. In juvenile *P. discolor*, enrichment of FoxP2 in layer 6 could be observed, but this varied across cortical areas (rostral-caudal and dorso-ventral). To illustrate this variation across the cortex, we

compared expression in juvenile and adult at four different rostral-caudal depths, and four different dorsal-ventral positions per depth (Figures 7-10). FoxP2 positive neurons were abundant at a number of positions in the juvenile cortex (e.g. Figure 8a1-b1, Figure 9a1-b1, Figure 10b1-d1), but only sparse FoxP2 positive layer 6 neurons were observed in the adult (Figures 7-10, panels a2-d2). Some of the highest enrichment of layer 6 FoxP2 expression in the juvenile auditory cortex was found in regions that roughly correspond to the posterior dorsal field (PDF, Figure 10b1) and the primary auditory cortex (Figure 10c1-d1) (Hoffmann et al., 2008). By comparison, staining was not visible in the primary auditory cortex of adult *P. discolor* (Figure 10b2-c2).

In both species, FoxP1 was observed across layers 2-6 (Figures 4-5, panels d-e), consistent with the rodent expression pattern (Figure 6b1). The staining appears weaker in the *R. aegyptiacus* cortex in Figure 5d-e, although high resolution images (see online database for *R. aegyptiacus*) clearly show that expression is present in a large number of neurons throughout the layers with a distribution comparable to *P. discolor* and mouse (see Figure S4d-e and Figure 6b-b1). Differences in intensity may be due to the different FoxP1 antibody used for *R. aegyptiacus* (see Table 1) since when this antibody was tested on *P. discolor* or mouse tissue, weaker staining was also observed in some parts of the cortex compared to other brain regions (data not shown). CntnaP2 was also expressed across layers 2-6 of the cortex of both species, with the strongest and most abundant expression found in layer 5 and sparse expression observed in other layers (Figures 4-5, panels f-g). This was consistent with the expression pattern of CntnaP2 observed in the mouse cortex (Figure 6c-c1).

Striatum

FoxP1 and FoxP2 showed strong and highly overlapping patterns of expression throughout the striatum, both being found abundantly in the caudate nucleus, putamen, nucleus accumbens, olfactory tubercle and lateral septal nucleus in both species (Figure 11). FoxP1 expression was never seen in the globus pallidus (Figure 11c-d), however intense staining of FoxP2 could be found, but only in very rare cells (Figure 11a-b). By comparison, CntnaP2 showed a largely inverse regional pattern of expression with only rare staining in the caudate nucleus and putamen, but abundant and intense staining in the globus pallidus and other regions of the pallidum (Figure 11e-f). Both weakly and intensely stained striatal neurons were observed for FoxP2 and FoxP1, which is of interest for future follow up since weak vs. intense FoxP2 levels have been related to age and singing behavior in songbirds (Thompson et al., 2013).

Hippocampus

The hippocampus was another region for which differences in FoxP2 expression were observed between the species. In *P. discolor*, FoxP2 was not expressed in the hippocampus, except for some very rare, mostly weak staining in CA1-3 (Figure 12a-f). However in *R. aegyptiacus*, FoxP2 was strongly and abundantly expressed in CA1 and the subiculum, but not found at all in other hippocampal regions (Figure 13a-f). Expression of FoxP1 and CntnaP2 was largely conserved across *P. discolor* and *R. aegyptiacus*. In both species, FoxP1 was abundantly found throughout neurons of CA1, CA2, CA3 and the subiculum (Figures 12-13, panels g-j). Staining in CA3 was weaker (Figures 12-13, panel i) compared to the very strong staining observed in the other regions. In both species CntnaP2 staining was strong and abundant throughout the hippocampus (Figures 12-13, panels k-n). A small difference was observed between the species in that CntnaP2 could be found in some rare cells of the subiculum in *P. discolor*, but not in *R. aegyptiacus*.

Thalamus

Staining in the Thalamus was largely conserved across both species (Figure 14-15), with a few exceptions in the ventral nuclear (differences in all 3 genes) and geniculate (differences in CntnaP2) groups of nuclei. FoxP2 expression was widespread and intense in the thalamus, being most abundant in the lateral, midline, ventral, intralaminar and geniculate nuclei (Figures 14-15, panels a, b, c1, d1, e1). A small species difference could be observed in the ventroposterolateral nucleus of the ventral nuclear group where abundant, moderate intensity expression was observed in *P. discolor*, but no expression was found in *R. aegyptiacus*. FoxP1 was also found throughout the thalamus often overlapping with FoxP2 expression. Although FoxP1 was generally less abundant and less intense in its staining pattern than FoxP2 (Figures 14-15, panels c2, d2, e2), it is possible that this is due to antibody/epitope differences. CntnaP2 was abundantly expressed in both species throughout the nuclei of the thalamus (Figures 14-15, panels c3, d3, e3). One clear CntnaP2 expression difference between the species was found in the geniculate group of nuclei, where CntnaP2 was abundant in almost all nuclei in *P. discolor*, but absent in all but the ventral lateral geniculate nucleus in *R. aegyptiacus*.

Amygdala

In the amygdala, FoxP1 and FoxP2 tended to show inverse patterns of expression (Figure 16 c-j, c1-j1 and Figure 17c-h, c1-h1). In both species, FoxP2 expression was low in the anterior lateral amygdaloid nucleus (La; Figure 16c and Figure 17c), where FoxP1 expression was high (Figure 16c1- and Figure

17c1). Conversely FoxP2 expression was high but FoxP1 expression was low in the anterior basolateral (BLa; Figure 16e-e1) or basal amygdaloid nuclei (Bmg; Figure 17d-d1), medial amygdaloid nucleus (Me) (Figure 16h-h1 and Figure 17g-g1), and intercalated amygdaloid nucleus (IA) (Figure 16i-i1 and Figure 17e-e1). FoxP1 and FoxP2 were both expressed in the central amygdaloid nucleus (Ce) (Figure 16g-g1 and Figure 17f-f1). CntnaP2 was not strongly expressed in the amygdala (Figure 16c2-j2 and Figure 17c2-h2), except for in a few regions in *R.aegyptiacus* including the La (Figure 17c2), Me (Figure 17g2) and accessory basal amygdaloid nucleus (AB) (Figure 17h2). In contrast *P. discolor* CntnaP2 staining was weak and sparse in these regions.

Cerebellum

In both species, FoxP2 was restricted to the Purkinje cell layer of the cerebellum (Figure 18c-d), whereas FoxP1 was not expressed at all in the cerebellum (Figure 18e-f). Cntnap2 was observed in Purkinje cells and in the granular layer, but not in cells of the molecular layer (Figure 18g-h). No species-specific differences were observed in the cerebellum for any of the genes tested.

Open access database of expression via the online 'Batlas' portal

All high resolution images are viewable via a persistent online open access database. This database contains the Nissl stained sections and the IHC staining for FoxP1, FoxP2 and CntnaP2 in two adult and one juvenile *P. discolor* and one adult *R. aegyptiacus* brain. The interactive database allows images to be browsed by species (*P. discolor* or *R. aegyptiacus*), age (adult or juvenile) or staining (FoxP1, FoxP2 CntnaP2 or Nissl staining) and have been meta-tagged to facilitate image searches based on these properties, on experimental conditions, or on the key brain regions represented in each image. These high resolution images allow viewing at high magnification (0.45-0.55 $\mu\text{m}/\text{pixel}$), making it possible to view expression at the level of individual neurons and observe the often subtle detail of expression patterns across brain regions. The BATLAS database can be accessed by the persistent link: <https://hdl.handle.net/1839/00-5B1D28A0-32AF-4DD4-8868-4404EC75EDAA@view> which will take browsers to the root of the database. To view images it is then necessary to either search the database for relevant tags (eg FoxP2, adult), or expand the file tree (via + symbol) to the relevant image or group of images (e.g. Batlas-> Bat Immuno-> *Phyllostomus discolor*-> Adult #1-> FoxP2-> Coronal-> *P. discolor* FoxP2-Banham).

DISCUSSION

To learn new vocalisations animals must identify and recognise relevant sounds, hold these sounds in memory as a vocal template, enact a motor program to mimic these sounds, use feedback to determine 'goodness of fit', and modify the motor output as appropriate to accurately match the template. As such, vocal production learning must, by necessity, involve multiple brain regions and neural circuits involved in sensorimotor perception, integration, memory and motor production (amongst others) (Brainard and Doupe, 2000; Mooney, 2009; Bolhuis et al., 2010). Although the neural circuits involved in bat vocal learning are not yet defined, work investigating these individual components and studies of vocal learning in songbirds, have highlighted regions of interest for mammalian vocal learning (Jarvis, 2007; Bolhuis et al., 2010; Petkov and Jarvis, 2012). Herein, we report detailed expression patterns of three key language-related genes in the brains of vocal learning bats. All three genes (FoxP2, FoxP1 and Cntna2) were expressed across many brain regions, but in specialised patterns within neuronal subtypes.

Forebrain circuits relevant for vocal learning – auditory circuitry

The auditory cortex is the region of the cortex primarily responsive to sound and the primary (AI) and anterior auditory (AAF) fields tend to have tonotopic organisations in mammals (Ehret, 1997; Rauschecker, 1998), including bats (Dear et al., 1993; Esser and Eiermann, 1999; Hoffmann et al., 2008; Ulanovsky and Moss, 2008). Audio-vocal control in bats and other mammals involves connections between the auditory cortex, anterior cingulate cortex (ACC), primary orofacial motor cortex and supplementary motor areas of the cortex as well as subcortical and midbrain regions (Jurgens, 2002; 2009; Loh et al., 2016; Roberts et al., 2017). While FoxP2 expression was strong in *R. aegyptiacus* cortex, including the auditory and anterior cingulate cortical areas, only sparse FoxP2 staining could be observed in the adult *P. discolor* cortex. In *P. discolor* juveniles however, cortical staining was strongly enriched in deep layers of the primary auditory cortex and posterior dorsal field (PDF) of the auditory cortex, suggesting that FoxP2 could play a role in postnatal development of these brain regions. Of note, the PDF of the *P. discolor* auditory cortex contains combination sensitive neurons that form a chronotopic map of echo delay (Greiter and Firzlauff, 2017). In the mustached bat (*Pteronotus parnellii*), neurons in comparable regions of the auditory cortex are specialised for processing communication calls (Ohlemiller et al., 1996) and are sensitive to the combinations of, and temporal relationships between, syllables of these calls (Ohlemiller et al., 1996; Esser et al., 1997). These data suggest there could be a

specific role for neurons in this FoxP2 positive region of the auditory cortex in processing temporal and syntactical information embedded in communication calls of bats.

The auditory cortex makes strong reciprocal connections to the auditory thalamus (the ventral medial geniculate nucleus; vMGN), which can dynamically shape auditory representations (Radtke-Schuller, 2004). In other bat species the dorsal fields of the auditory cortex receive connections from the dorsal medial geniculate body (dMGB) (Radtke-Schuller et al., 2004). The vMGN and auditory cortex have also been shown to be a major source of input to frontal motor cortex in the mustache bat (Kobler et al., 1987) and for *C. perspicillata*, a species closely related to *P. discolor*, neurons responsive to acoustic stimulation have been found in the frontal cortex (Eiermann and Esser, 2000). FoxP2 was strongly and abundantly expressed in the vMGN in both species, whereas FoxP1 was absent. CntnaP2 was strong and abundant in this region in *P. discolor*, but not in *R. aegyptiacus*. Together this may suggest that of these three genes, only FoxP2 is required in the auditory thalamus of both species.

The amygdala is important for evaluating incoming acoustic information and modulating the appropriate behavioural response (Gadziola et al., 2012). The lateral nucleus of the amygdala receives auditory information from the auditory cortex and vMGN and has direct connections back to the auditory cortex (Amaral and Price, 1984; LeDoux et al., 1991). In bats the lateral nucleus of the amygdala is important for discrimination of communication calls (Gadziola et al., 2012; Gadziola et al., 2016). In the lateral nucleus of the amygdala of both species FoxP1 showed strong and abundant staining, while Foxp2 was largely absent. CntnaP2 was strong and abundant in *R. aegyptiacus* but weak and sparse in *P. discolor*. As such we see an inverse pattern to what was observed in the vMGN, with FoxP1 appearing to be most important of the three genes for the lateral nucleus of the amygdala in both species.

Forebrain circuits relevant for vocal learning – vocal motor circuitry

FoxP2 has previously been observed to be strongly expressed throughout two cortical-subcortical loops controlling motor functions in mammals; the fronto-striatal and fronto-cerebellar circuits. This pattern of expression is largely conserved across rodents, non-human primates and the developing human brain, with only subtle differences observed across these highly evolutionarily distinct mammals (Ferland et al., 2003; Lai et al., 2003; Takahashi et al., 2003; 2008a; Takahashi et al., 2008b; Campbell et al., 2009; Hisaoka et al., 2010; Fujita and Sugihara, 2012; Kato et al., 2014). Because these circuits also underlie speech production, a crucial role for Foxp2 has been hypothesised in motor function and human speech

(Vargha-Khadem et al., 2005). Humans with heterozygous disruptions of *FOXP2* display motor dysfunctions that are largely localised to the vocal-motor domain (Lai et al., 2001; Watkins et al., 2002) with corresponding neuro-pathology in regions of the brain showing high *FOXP2* expression, including the striatum (Lai et al., 2003).

In songbirds, *FoxP2* is highly expressed in the song learning circuitry (which resembles the frontal-striatal circuitry of mammals). Genetic reduction of *FoxP2* expression in a key component of this circuit known as area X (comparable to the mammalian striatum) resulted in juvenile animals that were less accurate at learning their songs, and in adults resulted in more variable song production (Haesler et al., 2007; Murugan et al., 2013), pointing to a key role in songbird vocal learning. Mice with heterozygous *Foxp2* mutations, matching those found in humans, show a specific deficit in motor learning and altered striatal plasticity (Groszer et al., 2008; French et al., 2011). Together these data from human, songbird and mouse suggest that pathways involving the striatum and contributing to motor learning, vocal learning and vocal-motor control are particularly sensitive to reductions in *FoxP2* expression. Our data showed that *FoxP2* is found in equivalent motor-related regions (cortico-striatal and cortico-cerebellar circuits - with the exception of the cortex in adult *P. discolor*) and strongly expressed in the striatum of both bats. Given the precise motor control needed for bat flight, their highly gregarious nature, and their reliance on vocalisations for both social interactions and navigation, we predict that *FoxP2* expression in these circuits is likely to contribute to bat motor function and vocal control.

FOXP1 is involved in a range of neurodevelopmental phenotypes, including but not limited to speech and language. Children with *FOXP1* mutations display deficits including general motor delay, mild to moderate cognitive impairment, speech/language problems and autistic characteristics (Hamdan et al., 2010; Horn, 2011; O'Roak et al., 2011; Le Fevre et al., 2013; Lozano et al., 2015). *FoxP1* and *Foxp2* show highly overlapping patterns of expression and are known to function as dimers to co-regulate some genes (Ferland et al., 2003; Li et al., 2004; Teramitsu, 2004; Bacon and Rappold, 2012), as such this broader profile in affected individuals may be related to the wider distribution of *FOXP1* in the cortex and subsequent effects on cortical circuit development and function when its expression is reduced. In rodent and primate studies, *Foxp1* has a widespread pattern of expression, usually being found across layers 2-6 and this was also true for bat *FoxP1* (Ferland et al., 2003; Hisaoka et al., 2010; Kato et al., 2014). Loss of *Foxp1* in mice is embryonic lethal, however a brain specific knockout produced mice with behavioural impairments reflecting some of the human phenotypes including impaired short term

memory, hyperactivity, increased repetitive behaviour and reduced social interactions (Bacon et al., 2015). This was coupled with dramatic effects on striatal and hippocampal development, suggesting that loss of FoxP1 expression in these regions could also contribute to the phenotypes resulting from *FoxP1* mutations in both humans and mice. Both bat species showed abundant FoxP1 expression across layers 2-6 of the cortex and also showed strong and abundant expression in the striatum and the hippocampus. This expression pattern was highly overlapping in both species and matched closely with what has been observed in other mammals. This suggests that while FoxP1 is likely to play a role in bat vocal-motor and vocal learning circuits, it is expected to have widespread effects beyond these circuits and may also contribute to general cognitive abilities and social interactions.

CNTNAP2 shows a complex but critical contribution to human neurodevelopment. Mutations in human *CNTNAP2* result in epilepsy, intellectual disability, autistic phenotypes and speech/language impairments (Strauss et al., 2006; Jackman et al., 2009; Gregor et al., 2011; O'Roak et al., 2011; Rodenas-Cuadrado et al., 2014; Rodenas-Cuadrado et al., 2016). Common variation in this gene has also been associated with language impairment, autism, and metrics of language development in the normal population (Alarcón et al., 2008; Arking et al., 2008; Bakkaloglu et al., 2008; Vernes et al., 2008; Peter et al., 2011; Whitehouse et al., 2011), suggesting that while complete disruption of this gene has severe and widespread effects on neurodevelopment, subtle variation in the gene could specifically affect speech, language and social communication related circuits. Knockout mice lacking *Cntnap2* had neuronal phenotypes like altered neuronal firing and seizures, but also displayed behavioural phenotypes including improved motor coordination, reduced social interactions, and increased repetitive behaviour (Penagarikano et al., 2011). As for the other genes tested, we observed expression of *CntnaP2* in multiple brain regions of both bats. In primate and rodent brains, *CntnaP2* is strongly expressed in the cortex (layers 2-5), striatum and thalamus (Abrahams et al., 2007; Alarcón et al., 2008; Kato et al., 2014; Rodenas-Cuadrado et al., 2014). In the human brain, enrichment has been reported in the frontal cortex Broca's area and other perisylvian brain regions, suggesting an important role in development of higher order cognitive functions including speech and language (Abrahams et al., 2007). The expression pattern observed for *CntnaP2* in these bats was similar to that seen in humans and rodents and expression of *CntnaP2* often showed an inverse pattern to that of FoxP2. For example, *Cntnap2* expression is very rare in the caudate-putamen, high in the globus pallidus and high in layer 5 of the cortex. FoxP2 was high in the caudate-putamen, very rare in the globus pallidus and highest in layer 6 of the cortex (except for the *P. discolor* cortex). Although their expression is not always mutually

exclusive (for example both are expressed in the Purkinje cell layer of the cerebellum), the inverse expression pattern generally expressed by these proteins is consistent with the role of FOXP2 as a repressor of CNTNAP2 expression (Vernes et al., 2008).

Both *Cntna2* and *Foxp1* remain strong candidates to contribute to bat vocal learning via their functions in the brain regions described above. In addition to this, their broader expression patterns and phenotypes caused by mutations (in comparison to *Foxp2*) means that they also represent candidates that could influence social behaviours. Given the extensive social groups in which bats live and their reliance on social (vocal) communication, they represent an interesting model to study the effects of these genes on the production of social vocalisations or social learning.

FoxP2 expression in the cortex shows a divergent pattern between the two bat species tested.

Foxp2 has shown strong enrichment in deep layers of the cortex in all mammals (rodents and non-human primates) tested to date (Ferland et al., 2003; Lai et al., 2003; Campbell et al., 2009; Hisaoka et al., 2010; Kato et al., 2014). Little information is available for adult human brain, but in embryos, human FOXP2 is similarly restricted to deep layers of the developing cortex (Lai et al., 2003). Our study showed that this deep layer enrichment was found in adult *R. aegyptiacus*, but not in the adult *P. discolor* cortex.

The role of *Foxp2* expression in the adult cortex is not well understood and in animal models, the requirement for FOXP2 in cortical neurons in adulthood has not yet been addressed. However the two bats investigated herein represent a naturally occurring 'experiment' in that we have one species, *R. aegyptiacus*, with strong deep layer cortex *Foxp2* expression and another, *P. discolor*, with very little *Foxp2* in the adult cortex. Given that both these species are thought to be vocal learners, it follows that maintaining strong cortical *Foxp2* expression into adulthood is not a universal feature of vocal learning animals. However, this broad conclusion should be tempered by the fact that we are still in the very early stages of understanding vocal learning in bats, the age at which it can occur, and the neural circuitry involved (Knornschild, 2014; Vernes, 2017). Importantly in both bat species the evidence for vocal learning comes from young animals (Esser, 1994; Prat et al., 2015) and until we determine if either species is capable of adult vocal learning, it would be premature to speculate on the consequences of adult cortical *Foxp2* expression in this process.

Interestingly *R. aegyptiacus* also showed enrichment of FoxP2 in layer 4 of the cortex, a property not shared with rodents or non-human primates (Campbell et al., 2009; Kato et al., 2014). While it would be possible to speculate on the function of this unusual layer 4 expression pattern in *R. aegyptiacus* bats, neurobehavioural work will be needed to determine if these neurons show altered properties or connectivity, or if the presence of FoxP2 in these neurons contributes to specific behaviours such as sensorimotor integration or vocal learning. In the future, functional and neuro-behavioural studies, such as targeted knockdown experiments, will be critical for understanding the function of FoxP2 in vocal-motor control and/or vocal learning in the developing and adult cortex and could help explain the distinctive expression patterns we find in these two vocal learning species.

Species specific differences in expression of FoxP2, FoxP1 and CntnaP2 across bats

In addition to the striking cortical expression difference observed across the two bat species, a few other differences in the distribution of FoxP2, FoxP1 and CntnaP2 were observed. In all animals tested to date FoxP2 has been largely absent from the hippocampus (Ferland et al., 2003; Lai et al., 2003; Takahashi et al., 2003; 2008a; Takahashi et al., 2008b; Campbell et al., 2009; Hisaoka et al., 2010; Fujita and Sugihara, 2012; Kato et al., 2014). This pattern was recapitulated in *P. discolor*, which displayed only some very rare, weak staining of cells in CA1-3. By contrast, FoxP2 was strongly and abundantly expressed in CA1 and the subiculum of the hippocampus of *R. aegyptiacus*. Given that CA1 is the major output pathway of the hippocampus and that place neurons have been identified in this region in *R. aegyptiacus* (Yartsev and Ulanovsky, 2013), this could reflect a role for FoxP2 in memory and/or navigation in this species however molecular and functional testing are crucial to test such hypotheses. Finally, small species specific differences were observed in the thalamus for all three genes. FoxP2 was expressed across much of the ventral nuclear group of *P. discolor* but absent from the equivalent region in *R. aegyptiacus*. In contrast, FoxP1 was more highly expressed in these nuclei in *R. aegyptiacus*. CntnaP2 was highly abundant in the geniculate group of thalamic nuclei in *P. discolor*, but absent in *R. aegyptiacus*. Cntnap2 was also highly expressed in a number of regions of the amygdala in *R. aegyptiacus*, but showed very little expression in *P. discolor*. Given that these are highly divergent species, these expression differences may reflect some of the phenotypic differences observed between these bats, however knock-out or knock-in experiments would be required to link expression patterns to functional outcomes.

Conclusion

FOXP2, *FOXP1* and *CNTNAP2* have been strongly implicated in the development and function of neural circuitry subserving human speech and language. We detailed the distribution of these genes across the brains of two highly social and vocal learning bat species. We found expression patterns that broadly reflected those seen in humans and other mammals. A notable exception was the sparse expression of *FoxP2* in the cortex of adult *P. discolor*, suggesting that adult *Foxp2* expression in the cortex may not be a universal feature of vocal learning mammals. This work highlights brain regions that may be important for vocal-motor or vocal learning behaviour in bats including areas of the auditory cortex, cingulate gyrus, basal ganglia, vMGN of the thalamus and lateral nuclei of the amygdala, pinpointing these areas for further study. Functional neurogenetic studies in these species will be of great value to understand the role of these genes in vocal-motor and vocal learning behaviour in mammals.

ABBREVIATIONS (in alphabetical order)

A	-	Amygdala
AAF	-	Anterior auditory field
AB	-	Accessory basal amygdaloid complex
ACC	-	Anterior Cingulate Cortex
AI	-	Primary auditory cortex
BLa	-	Basolateral amygdaloid nucleus, pars anterior
BLp	-	Basolateral amygdaloid nucleus, pars posterior
Bmg	-	Basal nucleus of the amygdala, magnocellular part
C	-	Caudate
Ce	-	Central amygdaloid nucleus
CL	-	Centrolateral nucleus
CM	-	Centromedial nucleus
Ctx	-	Cortex
DG	-	Dentate gyrus
GL	-	Granular layer
GP	-	Globus Pallidus
Hi	-	Hippocampus
Hy	-	Hypothalamus
IA	-	Intercalated amygdaloid nucleus
IC	-	Inferior colliculus
IHC	-	Immunohistochemistry
IO	-	Inferior Olives
La	-	Lateral amygdaloid nucleus, pars anterior
LD	-	Laterodorsal nucleus
LGd	-	lateral Geniculate nucleus, dorsal
LGV	-	lateral Geniculate nucleus, ventral
IHb	-	lateral Habenular nucleus
Lp	-	Lateral amygdaloid nucleus, pars posterior
MD	-	Mediodorsal nucleus
Me	-	Medial amygdaloid nucleus
mHb	-	medial Habenular nucleus
ML	-	Molecular layer
P	-	Putamen
PC	-	Paracentral nucleus
PCL	-	Purkinje cell layer
PDF	-	Posterior dorsal field
PV	-	Paraventricular nucleus
Re	-	nucleus of Reuniens
Rh	-	Rhomboidal nucleus
RT	-	Reticular nucleus
SC	-	Superior colliculus
Th	-	Thalamus
VA	-	Ventral anterior nucleus
VL	-	Ventrolateral nucleus
VM	-	Ventromedial nucleus
vMGN	-	ventral Medial geniculate nucleus
VPL	-	Ventroposterolateral nucleus

ACKNOWLEDGEMENTS

This work was funded by a Marie Curie Career Integration Grant (PCIG12-GA-2012-333978) and a Max Planck Research Group Grant both awarded to S.C.V., and a Human Frontiers Science Program (HFSP) Research grant (RGP0058/2016) awarded to S.C.V., M.Y., U.F.

CONFLICT OF INTEREST

The authors declare that they have no conflict of interest

ROLE OF AUTHORS

Study concept and design, and writing article: SCV.

Sample acquisition: PMRC, TAS, MY, UF and SCV.

Data acquisition and analysis of data: PMRC, JM, PD, LB and SCV.

Critical revision of the article: JM, PD, MY, TAS, UF and SCV.

Accepted

REFERENCES

- Abrahams BS, Tentler D, Perederiy JV, Oldham MC, Coppola G, Geschwind DH. 2007. Genome-wide analyses of human perisylvian cerebral cortical patterning. *Proc Natl Acad Sci U S A* 104(45):17849-17854.
- Alarcón M, Abrahams BS, Stone JL, Duvall JA, Perederiy JV, Bomar JM, Sebat J, Wigler M, Martin CL, Ledbetter DH, Nelson SF, Cantor RM, Geschwind DH. 2008. Linkage, Association, and Gene-Expression Analyses Identify CNTNAP2 as an Autism-Susceptibility Gene. *The American Journal of Human Genetics* 82(1):150-159.
- Amaral DG, Price JL. 1984. Amygdalo-cortical projections in the monkey (*Macaca fascicularis*). *J Comp Neurol* 230(4):465-496.
- Arking DE, Cutler DJ, Brune CW, Teslovich TM, West K, Ikeda M, Rea A, Guy M, Lin S, Cook EH, Chakravarti A. 2008. A common genetic variant in the neurexin superfamily member CNTNAP2 increases familial risk of autism. *Am J Hum Genet* 82(1):160-164.
- Bacon C, Rappold GA. 2012. The distinct and overlapping phenotypic spectra of FOXP1 and FOXP2 in cognitive disorders. *Hum Genet* 131(11):1687-1698.
- Bacon C, Schneider M, Le Magueresse C, Froehlich H, Sticht C, Gluch C, Monyer H, Rappold GA. 2015. Brain-specific Foxp1 deletion impairs neuronal development and causes autistic-like behaviour. *Mol Psychiatry* 20(5):632-639.
- Bakkaloglu B, O'Roak BJ, Louvi A, Gupta AR, Abelson JF, Morgan TM, Chawarska K, Klin A, Ercan-Sencicek AG, Stillman AA, Tanriover G, Abrahams BS, Duvall JA, Robbins EM, Geschwind DH, Biederer T, Gunel M, Lifton RP, State MW. 2008. Molecular cytogenetic analysis and resequencing of contactin associated protein-like 2 in autism spectrum disorders. *Am J Hum Genet* 82(1):165-173.
- Baron G, Stephan H, Frahm HD. 1996. *Comparative neurobiology in Chiroptera*. Basel ; Boston: Birkhäuser Verlag.
- Bolhuis JJ, Okanoya K, Scharff C. 2010. Twitter evolution: converging mechanisms in birdsong and human speech. *Nat Rev Neurosci* 11(11):747-759.
- Brainard MS, Doupe AJ. 2000. Auditory feedback in learning and maintenance of vocal behaviour. *Nat Rev Neurosci* 1(1):31-40.
- Brainard MS, Doupe AJ. 2013. Translating Birdsong: Songbirds as a Model for Basic and Applied Medical Research. *Annual Review of Neuroscience*, Vol 36 36:489-517.
- Campbell P, Reep RL, Stoll ML, Ophir AG, Phelps SM. 2009. Conservation and diversity of Foxp2 expression in muroid rodents: functional implications. *J Comp Neurol* 512(1):84-100.
- Condro MC, White SA. 2014. Distribution of language-related Cntnap2 protein in neural circuits critical for vocal learning. *J Comp Neurol* 522(1):169-185.
- Dear SP, Fritz J, Haresign T, Ferragamo M, Simmons JA. 1993. Tonotopic and functional organization in the auditory cortex of the big brown bat, *Eptesicus fuscus*. *J Neurophysiol* 70(5):1988-2009.
- Doupe AJ, Kuhl PK. 1999. Birdsong and human speech: common themes and mechanisms. *Annu Rev Neurosci* 22:567-631.
- Doupe AJ, Perkel DJ, Reiner A, Stern EA. 2005. Birdbrains could teach basal ganglia research a new song. *Trends Neurosci* 28(7):353-363.
- Doupe AJ, Solis MM, Kimpo R, Boettiger CA. 2004. Cellular, circuit, and synaptic mechanisms in song learning. *Ann N Y Acad Sci* 1016:495-523.
- Ehret G. 1997. The auditory cortex. *J Comp Physiol A* 181(6):547-557.
- Eiermann A, Esser KH. 2000. Auditory responses from the frontal cortex in the short-tailed fruit bat *Carollia perspicillata*. *Neuroreport* 11(2):421-425.

- Esser KH. 1994. Audio-vocal learning in a non-human mammal: the lesser spear-nosed bat *Phyllostomus discolor*. *Neuroreport* 5(14):1718-1720.
- Esser KH, Condon CJ, Suga N, Kanwal JS. 1997. Syntax processing by auditory cortical neurons in the FM-FM area of the mustached bat *Pteronotus parnellii*. *Proc Natl Acad Sci U S A* 94(25):14019-14024.
- Esser KH, Eiermann A. 1999. Tonotopic organization and parcellation of auditory cortex in the FM-bat *Carollia perspicillata*. *Eur J Neurosci* 11(10):3669-3682.
- Esser KH, Kiefer R. 1996. Detection of frequency modulation in the FM-bat *Phyllostomus discolor*. *J Comp Physiol [A]* 178(6):787-796.
- Esser KH, Schmidt U. 1989. Mother-Infant Communication in the Lesser Spear-Nosed Bat *Phyllostomus discolor* (Chiroptera, Phyllostomidae) - Evidence for Acoustic Learning. *Ethology* 82(2):156-168.
- Esser KH, Schmidt U. 1990. Behavioral auditory thresholds in neonate lesser spear-nosed bats, *Phyllostomus discolor*. *Naturwissenschaften* 77(6):292-294.
- Ferland RJ, Cherry TJ, Preware PO, Morrissey EE, Walsh CA. 2003. Characterization of *Foxp2* and *Foxp1* mRNA and protein in the developing and mature brain. *J Comp Neurol* 460(2):266-279.
- Fisher SE, Scharff C. 2009. *FOXP2* as a molecular window into speech and language. *Trends Genet* 25(4):166-177.
- French CA, Jin X, Campbell TG, Gerfen E, Groszer M, Fisher SE, Costa RM. 2011. An aetiological *Foxp2* mutation causes aberrant striatal activity and alters plasticity during skill learning. *Mol Psychiatry* 17(11):1077-1085.
- Fujita H, Sugihara I. 2012. *FoxP2* expression in the cerebellum and inferior olive: development of the transverse stripe-shaped expression pattern in the mouse cerebellar cortex. *J Comp Neurol* 520(3):656-677.
- Gadziola MA, Grimsley JM, Shanbhag SJ, Wenstrup JJ. 2012. A novel coding mechanism for social vocalizations in the lateral amygdala. *J Neurophysiol* 107(4):1047-1057.
- Gadziola MA, Shanbhag SJ, Wenstrup JJ. 2016. Two distinct representations of social vocalizations in the basolateral amygdala. *J Neurophysiol* 115(2):868-886.
- Goldstein MH, King AP, West MJ. 2003. Social interaction shapes babbling: testing parallels between birdsong and speech. *Proc Natl Acad Sci U S A* 100(13):8030-8035.
- Gordon A, Salomon D, Barak N, Pen Y, Tsoory M, Kimchi T, Peles E. 2016. Expression of *Cntnap2* (*Caspr2*) in multiple levels of sensory systems. *Mol Cell Neurosci* 70:42-53.
- Gregor A, Albrecht B, Bader I, Bijlsma EK, Ekici AB, Engels H, Hackmann K, Horn D, Hoyer J, Klappecki J, Kohlhasse J, Maystadt I, Nagl S, Prott E, Tinschert S, Ullmann R, Wohlleber E, Woods G, Reis A, Rauch A, Zweier C. 2011. Expanding the clinical spectrum associated with defects in *CNTNAP2* and *NRXN1*. *BMC Med Genet* 12:106.
- Greiter W, Firzlauff U. 2017. Echo-acoustic flow shapes object representation in spatially complex acoustic scenes. *J Neurophysiol* 117(6):2113-2124.
- Groszer M, Keays DA, Deacon RM, de Bono JP, Prasad-Mulcare S, Gaub S, Baum MG, French CA, Nicod J, Coventry JA, Enard W, Fray M, Brown SD, Nolan PM, Paabo S, Channon KM, Costa RM, Eilers J, Ehret G, Rawlins JN, Fisher SE. 2008. Impaired synaptic plasticity and motor learning in mice with a point mutation implicated in human speech deficits. *Curr Biol* 18(5):354-362.
- Haesler S, Rochefort C, Georgi B, Licznarski P, Osten P, Scharff C. 2007. Incomplete and inaccurate vocal imitation after knockdown of *FoxP2* in songbird basal ganglia nucleus Area X. *PLoS Biol* 5(12):e321.
- Haesler S, Wada K, Nshdejan A, Morrissey EE, Lints T, Jarvis ED, Scharff C. 2004. *FoxP2* expression in avian vocal learners and non-learners. *J Neurosci* 24(13):3164-3175.
- Hamdan FF, Daoud H, Rochefort D, Piton A, Gauthier J, Langlois M, Foomani G, Dobrzyniecka S, Krebs MO, Joobor R, Lafreniere RG, Lacaille JC, Mottron L, Drapeau P, Beauchamp MH, Phillips MS,

- Fombonne E, Rouleau GA, Michaud JL. 2010. De novo mutations in FOXP1 in cases with intellectual disability, autism, and language impairment. *Am J Hum Genet* 87(5):671-678.
- Hevner RF. 2007. Layer-specific markers as probes for neuron type identity in human neocortex and malformations of cortical development. *J neuropath and exp neurol* 66(2):101-109.
- Hilliard AT, Miller JE, Fraley ER, Horvath S, White SA. 2012. Molecular microcircuitry underlies functional specification in a basal ganglia circuit dedicated to vocal learning. *Neuron* 73(3):537-552.
- Hisaoka T, Nakamura Y, Senba E, Morikawa Y. 2010. The forkhead transcription factors, Foxp1 and Foxp2, identify different subpopulations of projection neurons in the mouse cerebral cortex. *Neuroscience* 166(2):551-563.
- Hoffmann S, Firzlaff U, Radtke-Schuller S, Schwellnus B, Schuller G. 2008. The auditory cortex of the bat *Phyllostomus discolor*: Localization and organization of basic response properties. *BMC Neurosci* 9:65.
- Horn D. 2011. Mild to Moderate Intellectual Disability and Significant Speech and Language Deficits in Patients with FOXP1 Deletions and Mutations. *Molecular Syndromology*.
- Jabaudon D, Shnyder SJ, Tischfield DJ, Galazo MJ, Macklis JD. 2012. RORbeta induces barrel-like neuronal clusters in the developing neocortex. *Cereb Cortex* 22(5):996-1006.
- Jackman C, Horn ND, Molleston JP, Sokol DK. 2009. Gene associated with seizures, autism, and hepatomegaly in an Amish girl. *Pediatr Neurol* 40(4):310-313.
- Janik VM, Slater PJ. 2000. The different roles of social learning in vocal communication. *Anim Behav* 60(1):1-11.
- Janik VM, Slater PJB. 1997. Vocal learning in mammals. *Adv Stud Behav* 26:59-99.
- Jarvis ED. 2004. Learned birdsong and the neurobiology of human language. *Ann N Y Acad Sci* 1016:749-777.
- Jarvis ED. 2007. Neural systems for vocal learning in birds and humans: a synopsis. *J Ornithol* 148(1):35-44.
- Jurgens U. 2002. A study of the central control of vocalization using the squirrel monkey. *Med Eng Phys* 24(7-8):473-477.
- Jurgens U. 2009. The neural control of vocalization in mammals: a review. *J Voice* 23(1):1-10.
- Kato M, Okanoya K, Koike T, Sasaki E, Okano H, Watanabe S, Iriki A. 2014. Human speech- and reading-related genes display partially overlapping expression patterns in the marmoset brain. *Brain Lang* 133:26-38.
- Knornschild M. 2014. Vocal production learning in bats. *Curr Opin Neurobiol* 28C:80-85.
- Kobler JB, Isbey SF, Casseday JH. 1987. Auditory pathways to the frontal cortex of the mustache bat, *Pteronotus parnellii*. *Science* 236(4803):824-826.
- Lai CS, Fisher SE, Hurst JA, Vargha-Khadem F, Monaco AP. 2001. A forkhead-domain gene is mutated in a severe speech and language disorder. *Nature* 413(6855):519-523.
- Lai CS, Gerrelli D, Monaco AP, Fisher SE, Copp AJ. 2003. FOXP2 expression during brain development coincides with adult sites of pathology in a severe speech and language disorder. *Brain* 126(Pt 11):2455-2462.
- Le Fevre AK, Taylor S, Malek NH, Horn D, Carr CW, Abdul-Rahman OA, O'Donnell S, Burgess T, Shaw M, Gecz J, Bain N, Fagan K, Hunter MF. 2013. FOXP1 mutations cause intellectual disability and a recognizable phenotype. *Am J Med Genet A* 161A(12):3166-3175.
- LeDoux JE, Farb CR, Romanski LM. 1991. Overlapping projections to the amygdala and striatum from auditory processing areas of the thalamus and cortex. *Neurosci Lett* 134(1):139-144.
- Lein ES, Hawrylycz MJ, Ao N, Ayres M, Bensinger A, Bernard A, Boe AF, Boguski MS, Brockway KS, Byrnes EJ, Chen L, Chen TM, Chin MC, Chong J, Crook BE, Czaplinska A, Dang CN, Datta S, Dee NR, Desaki AL, Desta T, Diep E, Dolbeare TA, Donelan MJ, Dong HW, Dougherty JG, Duncan BJ, Ebbert AJ, Eichele G, Estin LK, Faber C, Facer BA, Fields R, Fischer SR, Fliss TP, Frensley C, Gates

- SN, Glattfelder KJ, Halverson KR, Hart MR, Hohmann JG, Howell MP, Jeung DP, Johnson RA, Karr PT, Kawal R, Kidney JM, Knapik RH, Kuan CL, Lake JH, Laramée AR, Larsen KD, Lau C, Lemon TA, Liang AJ, Liu Y, Luong LT, Michaels J, Morgan JJ, Morgan RJ, Mortrud MT, Mosqueda NF, Ng LL, Ng R, Orta GJ, Overly CC, Pak TH, Parry SE, Pathak SD, Pearson OC, Puchalski RB, Riley ZL, Rockett HR, Rowland SA, Royall JJ, Ruiz MJ, Sarno NR, Schaffnit K, Shapovalova NV, Sivasay T, Slaughterbeck CR, Smith SC, Smith KA, Smith BI, Sodt AJ, Stewart NN, Stumpf KR, Sunkin SM, Sutram M, Tam A, Teemer CD, Thaller C, Thompson CL, Varnam LR, Visel A, Whitlock RM, Wohnoutka PE, Wolkey CK, Wong VY, Wood M, Yaylaoglu MB, Young RC, Youngstrom BL, Yuan XF, Zhang B, Zwingman TA, Jones AR. 2007. Genome-wide atlas of gene expression in the adult mouse brain. *Nature* 445(7124):168-176.
- Li S, Weidenfeld J, Morrisey EE. 2004. Transcriptional and DNA binding activity of the Foxp1/2/4 family is modulated by heterotypic and homotypic protein interactions. *Mol Cell Biol* 24(2):809-822.
- Loh KK, Petrides M, Hopkins WD, Procyk E, Amiez C. 2016. Cognitive control of vocalizations in the primate ventrolateral-dorsomedial frontal (VLF-DMF) brain network. *Neurosci Biobehav Rev*.
- Lozano R, Vino A, Lozano C, Fisher SE, Deriziotis P. 2015. A de novo FOXP1 variant in a patient with autism, intellectual disability and severe speech and language impairment. *Eur J Hum Genet* 23(12):1702-1707.
- Mello CV. 2002. Mapping vocal communication pathways in birds with inducible gene expression. *J Comp Physiol A Neuroethol Sens Neural Behav Physiol* 188(11-12):943-959.
- Mooney R. 2009. Neural mechanisms for learned birdsong. *Learn Mem* 16(11):655-669.
- Morgan A FS, Scheffer I, et al. 2016. FOXP2-Related Speech and Language Disorders. *GeneReviews*® <https://www.ncbi.nlm.nih.gov/books/NBK368474/>.
- Moroni RF, Inverardi F, Regondi MC, Watakabe A, Yamamori T, Spreafico R, Frassoni C. 2009. Expression of layer-specific markers in the adult neocortex of BCNU-Treated rat, a model of cortical dysplasia. *Neuroscience* 159(2):682-691.
- Murugan M, Harward S, Scharff C, Mooney R. 2013. Diminished FoxP2 levels affect dopaminergic modulation of corticostriatal signaling important to song variability. *Neuron* 80(6):1464-1476.
- Nakagawa JM, Donkels C, Fauser S, Schulze-Bonhage A, Prinz M, Zentner J, Haas CA. 2017. Characterization of focal cortical dysplasia with balloon cells by layer-specific markers: Evidence for differential vulnerability of interneurons. *Epilepsia* 58(4):635-645.
- O'Roak BJ, Deriziotis P, Lee C, Vives L, Schwartz JJ, Girirajan S, Karakoc E, Mackenzie AP, Ng SB, Baker C, Rieder MJ, Nickerson DA, Bernier R, Fisher SE, Shendure J, Eichler EE. 2011. Exome sequencing in sporadic autism spectrum disorders identifies severe de novo mutations. *Nat Genet* 43(6):585-589.
- Ohlemiller KK, Kanwal JS, Suga N. 1996. Facilitative responses to species-specific calls in cortical FM-FM neurons of the mustached bat. *Neuroreport* 7(11):1749-1755.
- Panaitof SC, Abrahams BS, Dong H, Geschwind DH, White SA. 2010. Language-related Cntnap2 gene is differentially expressed in sexually dimorphic song nuclei essential for vocal learning in songbirds. *J Comp Neurol* 518(11):1995-2018.
- Penagarikano O, Abrahams BS, Herman EI, Winden KD, Gdalyahu A, Dong H, Sonnenblick LI, Gruver R, Almajano J, Bragin A, Golshani P, Trachtenberg JT, Peles E, Geschwind DH. 2011. Absence of CNTNAP2 leads to epilepsy, neuronal migration abnormalities, and core autism-related deficits. *Cell* 147(1):235-246.
- Peter B, Raskind WH, Matsushita M, Lisowski M, Vu T, Berninger VW, Wijsman EM, Brkanac Z. 2011. Replication of CNTNAP2 association with nonword repetition and support for FOXP2 association with timed reading and motor activities in a dyslexia family sample. *J Neurodev Disord* 3(1):39-49.

- Petkov CI, Jarvis ED. 2012. Birds, primates, and spoken language origins: behavioral phenotypes and neurobiological substrates. *Front Evol Neurosci* 4:12.
- Prat Y, Taub M, Yovel Y. 2015. Vocal learning in a social mammal: Demonstrated by isolation and playback experiments in bats. *Science Advances* 1(2):e1500019.
- Radtke-Schuller S. 2004. Cytoarchitecture of the medial geniculate body and thalamic projections to the auditory cortex in the rufous horseshoe bat (*Rhinolophus rouxi*). I. Temporal fields. *Anat Embryol (Berl)* 209(1):59-76.
- Radtke-Schuller S, Schuller G, O'Neill WE. 2004. Thalamic projections to the auditory cortex in the rufous horseshoe bat (*Rhinolophus rouxi*). II. Dorsal fields. *Anat Embryol (Berl)* 209(1):77-91.
- Rauschecker JP. 1998. Cortical processing of complex sounds. *Curr Opin Neurobiol* 8(4):516-521.
- Roberts TF, Hisey E, Tanaka M, Kearney MG, Chattree G, Yang CF, Shah NM, Mooney R. 2017. Identification of a motor-to-auditory pathway important for vocal learning. *Nat Neurosci*.
- Rodenas-Cuadrado P, Ho J, Vernes SC. 2014. Shining a light on CNTNAP2: complex functions to complex disorders. *Eur J Hum Genet* 22(2):171-178.
- Rodenas-Cuadrado P, Pietrafusa N, Francavilla T, La Neve A, Striano P, Vernes SC. 2016. Characterisation of CASPR2 deficiency disorder - a syndrome involving autism, epilepsy and language impairment. *BMC Med Genet* 17(1):8.
- Scalia F. 2013. Forebrain atlas of the short-tailed fruit bat, *carollia perpicillata* : prepared by the methods of nissl and neuron immunohistochemistry. pages cm p.
- Scharff C, White SA. 2004. Genetic components of vocal learning. *Ann N Y Acad Sci* 1016:325-347.
- Schneider R. 1966. Das Gehirn von *Rousettus aegyptiacus* (E. Geoffroy 1810) (Megachiroptera, Chiroptera, Mammalia). Ein mit Hilfe mehrerer Schnittserien erstellter Atlas. *Abhandlungen der Senckenbergischen naturforschenden Gesellschaft* 513:1-160.
- Sollis E, Graham SA, Vano A, Froehlich H, Vreeburg M, Dimitropoulou D, Gilissen C, Pfundt R, Rappold GA, Brunner HG, Deriziotis P, Fisher SE. 2016. Identification and functional characterization of de novo FOXP1 variants provides novel insights into the etiology of neurodevelopmental disorder. *Hum Mol Genet* 25(3):546-557.
- Strauss KA, Puffenberger EG, Huentelman MJ, Gottlieb S, Dobrin SE, Parod JM, Stephan DA, Morton DH. 2006. Recessive symptomatic focal epilepsy and mutant contactin-associated protein-like 2. *N Engl J Med* 354(13):1370-1377.
- Takahashi K, Liu FC, Hirokawa K, Takahashi H. 2003. Expression of Foxp2, a gene involved in speech and language, in the developing and adult striatum. *J Neurosci Res* 73(1):61-72.
- Takahashi K, Liu FC, Hirokawa K, Takahashi H. 2008a. Expression of Foxp4 in the developing and adult rat forebrain. *J Neurosci Res* 86(14):3106-3116.
- Takahashi K, Liu FC, Oishi T, Mori T, Higo N, Hayashi M, Hirokawa K, Takahashi H. 2008b. Expression of FOXP2 in the developing monkey forebrain: comparison with the expression of the genes FOXP1, PBX3, and MEIS2. *J Comp Neurol* 509(2):180-189.
- Tanimoto H, Teramitsu I, Poopatanapong A, Torrisi S, White SA. 2010. Striatal FoxP2 Is Actively Regulated during Songbird Sensorimotor Learning. *PLoS One* 5(1):e8548.
- Teeling EC, Springer MS, Madsen O, Bates P, O'Brien S J, Murphy WJ. 2005. A molecular phylogeny for bats illuminates biogeography and the fossil record. *Science* 307(5709):580-584.
- Teramitsu I. 2004. Parallel FoxP1 and FoxP2 Expression in Songbird and Human Brain Predicts Functional Interaction. *Journal of Neuroscience* 24(13):3152-3163.
- Teramitsu I. 2006. FoxP2 Regulation during Undirected Singing in Adult Songbirds. *Journal of Neuroscience* 26(28):7390-7394.
- Thompson CK, Schwabe F, Schoof A, Mendoza E, Gampe J, Rochefort C, Scharff C. 2013. Young and intense: FoxP2 immunoreactivity in Area X varies with age, song stereotypy, and singing in male zebra finches. *Front Neural Circuits* 7:24.

- Ulanovsky N, Moss CF. 2008. What the bat's voice tells the bat's brain. *Proc Natl Acad Sci U S A* 105(25):8491-8498.
- Vargha-Khadem F, Gadian DG, Copp A, Mishkin M. 2005. FOXP2 and the neuroanatomy of speech and language. *Nat Rev Neurosci* 6(2):131-138.
- Vernes SC. 2017. What bats have to say about speech and language. *Psychon Bull Rev* 24(1):111-117.
- Vernes SC, Newbury DF, Abrahams BS, Winchester L, Nicod J, Groszer M, Alarcon M, Oliver PL, Davies KE, Geschwind DH, Monaco AP, Fisher SE. 2008. A functional genetic link between distinct developmental language disorders. *N Engl J Med* 359(22):2337-2345.
- Watkins KE, Dronkers NF, Vargha-Khadem F. 2002. Behavioural analysis of an inherited speech and language disorder: comparison with acquired aphasia. *Brain* 125(Pt 3):452-464.
- White SA, Fisher SE, Geschwind DH, Scharff C, Holy TE. 2006. Singing mice, songbirds, and more: models for FOXP2 function and dysfunction in human speech and language. *J Neurosci* 26(41):10376-10379.
- Whitehouse AJ, Bishop DV, Ang QW, Pennell CE, Fisher SE. 2011. CNTNAP2 variants affect early language development in the general population. *Genes Brain Behav* 10(4):451-456.
- Yartsev MM, Ulanovsky N. 2013. Representation of three-dimensional space in the hippocampus of flying bats. *Science* 340(6130):367-372.
- Yovel Y, Geva-Sagiv M, Ulanovsky N. 2011. Click-based echolocation in bats: not so primitive after all. *J Comp Physiol A Neuroethol Sens Neural Behav Physiol* 197(5):515-530.

Accepted

FIGURE LEGENDS

Figure 1. Histological sections displaying the cytoarchitecture of the *P. discolor* bat brain. The collection of 49 coronal plane sections of the *P. discolor* bat brain used for histology, arranged anterior to posterior. The 4 μm thick sections shown in this figure were Nissl stained to show the cytoarchitecture of the bat brain, and adjacent 4 μm sections were used for IHC (shown in subsequent figures) to determine the expression patterns of FoxP2, FoxP1 and Cntnap2. Representative tissue sections used for detailed analysis are indicated by an asterisk below the relevant brain slice. Scale bar represents 4 mm.

Figure 2. Histological sections displaying the cytoarchitecture of the *R. aegyptiacus* bat brain. The collection of 45 coronal plane sections (single hemisphere) of the *R. aegyptiacus* bat brain used for histology, arranged anterior to posterior. The 4 μm thick sections shown in this figure were Nissl stained to show the cytoarchitecture of the brain, and adjacent 4 μm sections were used for IHC (shown in main figures) to determine the expression patterns of FoxP2, FoxP1 and Cntnap2. Representative tissue sections used for detailed analysis are indicated by an asterisk below the relevant section. Scale bar represents 4 mm.

Figure 3. Whole dissected bat brains indicating depths of slices used for representative images. Side view of the *P. discolor* and *R. aegyptiacus* adult brains following whole brain dissection. The approximate brain depths used to display representative images in the main figures are indicated by the black lines.

Figure 4. Examination of the *P. discolor* cortex reveals layer and species specific expression patterns. Structural overview of the *P. discolor* brain slice (immunostained against FoxP2) used to select inset boxes, including simplified line diagrams indicating key brain regions represented (a). See Figure 3 for an indication of slice depth. Inset boxes demonstrate representative immunostaining for FoxP2 (b-c), FoxP1 (d-e) and CntnaP2 (f-g). Note that FoxP2 and FoxP1 display nuclear localised staining, while Cntnap2 (Caspr2) displays a cytoplasmic/cell surface pattern of localisation. High magnification panels for each gene (c,e,g) were included to facilitate visualisation of details. Scale bar in panel (a) represents 1 mm, scale bars in (b, d, f) represent 250 μm and in (c, e, g) represent 125 μm . Red arrows indicate examples

of positively stained cells. Brain structures are abbreviated as follows; Cortex (Ctx), Caudate (C), Putamen (P), Globus Pallidus (GP), Thalamus (Th) and Hypothalamus (Hy).

Figure 5. Examination of the *R. aegyptiacus* cortex reveals layer and species specific expression patterns. Structural overview of the *R. aegyptiacus* brain slices (immunostained against FoxP2) used to select inset boxes, including simplified line diagrams indicating key brain regions represented (a). See Figure 3 for an indication of slice depth. Inset boxes demonstrate representative immunostaining for FoxP2 (b-c), FoxP1 (d-e) and CntnaP2 (f-g). High magnification panels for each gene (c, e, g) were included to facilitate visualisation of details. Scale bar in panel (a) represents 1 mm, scale bars in (b, d, f) represent 250 μm and in (c, e, g) represent 125 μm . Red arrows indicate examples of positively stained cells. Brain structures are abbreviated as follows; Cortex (Ctx), Caudate (C), Putamen (P), Globus Pallidus (GP), Thalamus (Th) and Hypothalamus (Hy).

Figure 6. Cortical layering is conserved between mouse brains and *P. discolor* bats. *P. discolor* (a-e) and *M. musculus* (a1-e1) brains were stained for FoxP2 (a-a1), FoxP1 (b-b1) and CntnaP2 (c-c1). The pattern of standard cortical markers was also compared across species including RorB - a layer 4 cortical marker (d-d1) and TLE4 - a layer 6 cortical marker (e-e1). Dotted lines represent boundaries between the cortical layers that were determined based on RorB and TLE4 expression, as well as cellular morphology. All genes and layer markers showed consistent distribution in the cortex across mouse and *P. discolor*, except for FoxP2. Scale bar represents 250 μm .

Figure 7. Distribution of FoxP2 in layer 6 of the juvenile vs. adult *P. discolor* cortex. Anterior brain slice (rostral-caudal distance $\sim 3,700 \mu\text{m}$) was chosen to illustrate representative FoxP2 protein expression in this cortical region which roughly corresponds to the location of the somatosensory cortex in other bat species. Comparable depths were used for both juvenile (~ 2.5 months old) and adult (>1 year old) brains. Inset boxes (a-d) indicate the location of the high magnification images for juvenile (a1-d1) and adult (a2-d2) brains. Only rare and weak staining can be observed in these regions of the cortex in both juvenile and adult animals. Scale bar in left panel (a-d) represents 1 mm, and scale bars in panels a1-a2 represent 125 μm . Broken lines indicate the boundary between layer 6 (L6) and the corpus callosum. Red arrows show examples of positively stained cells.

Figure 8. Distribution of FoxP2 in layer 6 of the juvenile vs. adult *P. discolor* cortex. Anterior brain slice (rostral-caudal distance $\sim 5,900 \mu\text{m}$) was chosen to illustrate representative FoxP2 protein expression in this cortical region. Comparable depths were used for both juvenile (~ 2.5 months old) and adult (>1 year old) brains. Inset boxes (a-d) indicate the location of the high magnification images for juvenile (a1-d1) and adult (a2-d2) brains. The juvenile *P. discolor* cortex shows abundant layer 6 FoxP2 expression in section a1 and moderate expression in b1, compared to the rare layer 6 expression observed in the comparable adult sections (a2, b2). Only rare expression was observed in juvenile (c1-d1) or adult (c2-d2) in other regions of the cortex, which roughly correspond to the anterior dorsal and anterior ventral fields (ADF, AVF) of the auditory cortex in *P. discolor*. The ADF is non-tonotopically organized and contains neurons mainly tuned to frequencies of the echolocation calls of *P. discolor* (40-90kHz). The AVF is tonotopically organized with the frequency gradient running opposite to the gradient in primary auditory cortex (i.e. low frequencies are located at the rostral border). The AVF might represent the anterior auditory field described in other mammals (Hoffmann et al., 2008). Regions a) and b) might be considered as secondary auditory areas adjacent to the ADF in *P. discolor* but have not been characterized anatomically or functionally, so far. Scale bar in left panel (a-d) represents 1 mm, and scale bars in panels a1-a2 represent $125 \mu\text{m}$. Broken lines indicate the boundary between layer 6 (L6) and the corpus callosum. Red arrows show examples of positively stained cells.

Figure 9. Distribution of FoxP2 in layer 6 of the juvenile vs. adult *P. discolor* cortex. Posterior brain slice (rostral-caudal distance $\sim 8,000 \mu\text{m}$) was chosen to illustrate representative FoxP2 protein expression in this cortical region. Comparable depths were used for both juvenile (~ 2.5 months old) and adult (>1 year old) brains. Inset boxes (a-d) indicate the location of the high magnification images for juvenile (a1-d1) and adult (a2-d2) brains. The juvenile *P. discolor* cortex shows strong and abundant layer 6 FoxP2 expression in section a1 and b1, compared to the rare layer 6 expression observed in the corresponding adult sections (a2, b2). Only rare expression was observed in juvenile (c1-d1) or adult (c2-d2) in other regions of the cortex at this depth. Regions a) and b) might be considered as secondary auditory areas adjacent to the posterior dorsal auditory field (PDF) in *P. discolor* but have not been characterized anatomically or functionally, so far. Scale bar in left panel (a-d) represents 1 mm, and scale bars in panels a1-a2 represent $125 \mu\text{m}$. Broken lines indicate the boundary between layer 6 (L6) and the corpus callosum. Red arrows show examples of positively stained cells.

Figure 10. Distribution of FoxP2 in layer 6 of the juvenile vs. adult *P. discolor* cortex. Posterior brain slice (rostral-caudal distance ~8,900 μm) was chosen to illustrate representative FoxP2 protein expression in this cortical region. Comparable depths were used for both juvenile (~2.5 months old) and adult (>1 year old) brains. Inset boxes (a-d) indicate the location of the high magnification images for juvenile (a1-d1) and adult (a2-d2) brains. Juvenile (a1) and adult (a2) *P. discolor* regions show little FoxP2 expression in region (a) of the cortex at this depth. The juvenile *P. discolor* cortex shows strong and abundant layer 6 FoxP2 expression in sections b1 and c1 and moderate expression in d1. No FoxP2 positive cells could be found in corresponding adult brain regions (b2-d2). Region (b) roughly corresponds to the posterior dorsal field (PDF) of the auditory cortex and regions (c-d) roughly correspond to the primary auditory cortex of *P. discolor*. Scale bar in left panel (a-d) represents 1 mm, and scale bars in panels a1-a2 represent 125 μm . Broken lines indicate the boundary between layer 6 (L6) and the corpus callosum. Red arrows show examples of positively stained cells.

Figure 11. FoxP genes show an inverse expression pattern to CntnaP2 in compartments of the striatum of both bat species. High magnification images were taken from the brain slices at the depth indicated in Figure 3, which is the same depth as for Figure 4 (*P. discolor*) and 5 (*R. aegyptiacus*). Representative IHC images for FoxP2 (a-b) and FoxP1 (c-d) demonstrate strong expression in the putamen, but not in the globus pallidus. Conversely CntnaP2 is strongly expressed in the globus pallidus but not in the putamen (e-f). Broken lines illustrate the boundary between putamen and globus pallidus and red arrows indicate examples of positively stained cells. Scale bars represent 125 μm for *P. discolor* panels (a, c, e) and 250 μm for *R. aegyptiacus* panels (b, d, f).

Figure 12. Distribution of FoxP2, FoxP1 and CntnaP2 in the hippocampus of *P. discolor*. Structural overview of the *P. discolor* brain slice (immunostained against FoxP2) used to select inset boxes, including simplified line diagrams indicating key brain regions represented (a). See Figure 3 for an indication of slice depth. Higher magnification of the hippocampus (b) shows further black inset boxes representing highest magnification insets detailing the CA1, CA2, CA3 and DG regions. FoxP2 shows little expression in the hippocampus besides rare neurons (c-f). FoxP1 is consistently expressed in CA1-3 (g-j) and CntnaP2 in CA1-3 and the DG (k-n). Scale bar in panel (a) represents 1 mm, panel (b) represents 250 μm , and scale bars in panel's (c-n) represent 200 μm . Brain structures are abbreviated as follows; Cortex (Ctx), Thalamus (Th), Hypothalamus (Hy) and hippocampus (Hi). Red arrows indicate examples of positively stained cells.

Figure 13. Distribution of FoxP2, FoxP1 and CntnaP2 in the hippocampus of *R. aegyptiacus*. Structural overview of the *P. discolor* brain slice (immunostained against FoxP2) used to create inset boxes, including simplified line diagrams indicating key brain regions represented (a). See Figure 3 for an indication of slice depth. Higher magnification of the hippocampus (b) shows further black inset boxes representing highest magnification insets detailing the CA1, CA2, CA3 and DG regions. FoxP2 is expressed in the CA1 region (c), but not in any other region of the hippocampus (d-f). FoxP1 is consistently expressed in CA1-3 (g-j) and CntnaP2 in CA1-3 and the DG (k-n). Scale bar in panel (a) represents 2 mm, panel (b) represents 500 μm , and scale bars in panels (c-n) represent 200 μm . Brain structures are abbreviated as follows; Cortex (Ctx), Thalamus (Th), Hypothalamus (Hy) and hippocampus (Hi). Red arrows indicate examples of positively stained cells.

Figure 14. Distribution of FoxP2, FoxP1 and CntnaP2 in the thalamus of *P. discolor*. Structural overview of the *P. discolor* brain slice (immunostained against FoxP2) including simplified line diagrams indicating key brain regions (a), used to select inset boxes (b). See Figure 3 for an indication of slice depth. High magnification images display expression patterns of FoxP2 (c1, d1, e1), FoxP1 (c2, d2, e2) and CntnaP2 (c3, d3, e3). Scale bar in panel (a) represents 1 mm, panel (b) represents 500 μm , and scale bars in panels (c1-e3) can be found in (c1, b1 and c1) and represent 250 μm . Brain structures are abbreviated as follows: Cortex (Ctx), Caudate (C), Putamen (P), Thalamus (Th), Hypothalamus (Hy), Hippocampus (Hi) and Amygdala (A). Thalamic nuclei are abbreviated as follows: Centrolateral nucleus (CL), Centromedial nucleus (CM), Laterodorsal nucleus (LD), lateral Habenular nucleus (lHb), lateral Geniculate nucleus, dorsal (LGd), lateral Geniculate nucleus, ventral (LGv), Mediodorsal nucleus (MD), medial Habenular nucleus (mHb), Paracentral nucleus (PC), Paraventricular nucleus (PV), Rhomboidal nucleus (Rh), nucleus of Reuiens (Re), Reticular nucleus (RT), Ventral anterior nucleus (VA), Ventrolateral nucleus (VL), Ventromedial nucleus (VM) and Ventroposterolateral nucleus (VPL). Red arrows indicate examples of positively stained cells.

Figure 15. Distribution of FoxP2, FoxP1 and CntnaP2 in the thalamus of *R. aegyptiacus*. Structural overview of the *R. aegyptiacus* brain slice (immunostained against FoxP2) including simplified line diagrams indicating key brain regions (a), used to select inset boxes (b). See Figure 3 for an indication of slice depth. High magnification images display expression patterns of FoxP2 (c1, d1, e1), FoxP1 (c2, d2, e2) and CntnaP2 (c3, d3, e3). Scale bar in panel (a) represents 1 mm, panel (b) represents 500 μm , and

scale bars in panels (c1-e3) can be found in (c1, b1 and c1) and represent 250 μm . Brain structures are abbreviated as follows: Cortex (Ctx), Caudate (C), Putamen (P), Thalamus (Th), Hypothalamus (Hy), Hippocampus (Hi) and Amygdala (A). Thalamic nuclei are abbreviated as follows: Centrolateral nucleus (CL), Centromedial nucleus (CM), Laterodorsal nucleus (LD), lateral Habenular nucleus (IHb), lateral Geniculate nucleus, dorsal (LGd), lateral Geniculate nucleus, ventral (LGv), Mediodorsal nucleus (MD), medial Habenular nucleus (mHb), Paracentral nucleus (PC), Paraventricular nucleus (PV), Rhomboidal nucleus (Rh), nucleus of Reuniens (Re), Reticular nucleus (RT), Ventral anterior nucleus (VA), Ventrolateral nucleus (VL), Ventromedial nucleus (VM) and Ventroposterolateral nucleus (VPL). Red arrows indicate examples of positively stained cells.

Figure 16. Distribution of FoxP2, FoxP1 and CntnaP2 in the amygdala of *P. discolor*. Structural overview of the *P. discolor* brain slice (immunostained against FoxP2) including simplified line diagrams indicating key brain regions used to select inset boxes (a). See Figure 3 for an indication of slice depth. Higher magnification image of the inset box (b) displays sub regions of the amygdala. Highest magnification images are shown for FoxP2 (c-j), FoxP1 (c1-j1) and CntnaP2 (c2-j2). Scale bar in panel (a) represents 1 mm, panel (b) represents 500 μm , and scale bars in panel's (c-j, c1-j1, c2-j2) represent 250 μm . Brain structures are abbreviated as follows; Lateral amygdaloid nucleus, pars anterior (La), Lateral amygdaloid nucleus, pars posterior (Lp), Basolateral amygdaloid nucleus, pars anterior (BLa), Basolateral amygdaloid nucleus, pars posterior (BLp), Central amygdaloid nucleus (Ce), Medial amygdaloid nucleus (Me), Intercalated amygdaloid nucleus (IA) and Accessory basal amygdaloid complex (AB). Red arrows indicate examples of positively stained cells.

Figure 17. Distribution of FoxP2, FoxP1 and CntnaP2 in the amygdala of *R. aegyptiacus*. Structural overview of the *R. aegyptiacus* brain slice (immunostained against FoxP2) used to select inset boxes (a), including simplified line diagrams indicating key brain regions represented. See Figure 3 for an indication of slice depth. Higher magnification image of the inset box (b) displays sub regions of the amygdala. Highest magnification images are shown for FoxP2 (c-h), FoxP1 (c1-h1) and CntnaP2 (c2-h2). Scale bar in panel (a) represents 1 mm, panel (b) represents 500 μm , and scale bars in panel's (c-h, c1-h1, c2-h2) represent 250 μm . Brain structures are abbreviated as follows; Cortex (Ctx), Caudate (C), Putamen (P), Thalamus (Th), Hypothalamus (Hy) and Amygdala (A). Amygdala sub regions are abbreviated as follows: Lateral amygdaloid nucleus, pars anterior (La), Basal nucleus of the amygdala, magnocellular part (Bmg),

Intercalated amygdaloid nucleus (IA), Central amygdaloid nucleus (Ce), Medial amygdaloid nucleus (Me), and Accessory basal amygdaloid complex (AB). Red arrows indicate examples of positively stained cells.

Figure 18. Distribution of FoxP2, FoxP1 and CntnaP2 in the cerebellum of *P. discolor* and *R. aegyptiacus*. Structural overview of the *P. discolor* (a) and *R. aegyptiacus* (b) brain slices (immunostained against FoxP2) used to create inset boxes. See Figure 3 for an indication of slice depth in each species. Inset images display that the expression patterns of FoxP2 (c-d), FoxP1 (e-f) and CntnaP2 (g-h) are highly conserved across species. High magnification images (c1-h1) were included to facilitate visualisation of fine detail. Scale bar in panels (a-b) represent 1 mm, panels (c-h) represent 125 μm , and scale bars in panels (c1-h1) represent 20 μm . Brain structures are abbreviated as follows; ML = molecular layer, PCL = Purkinje cell layer, GL = granular layer and red arrows indicate examples of positively stained cells.

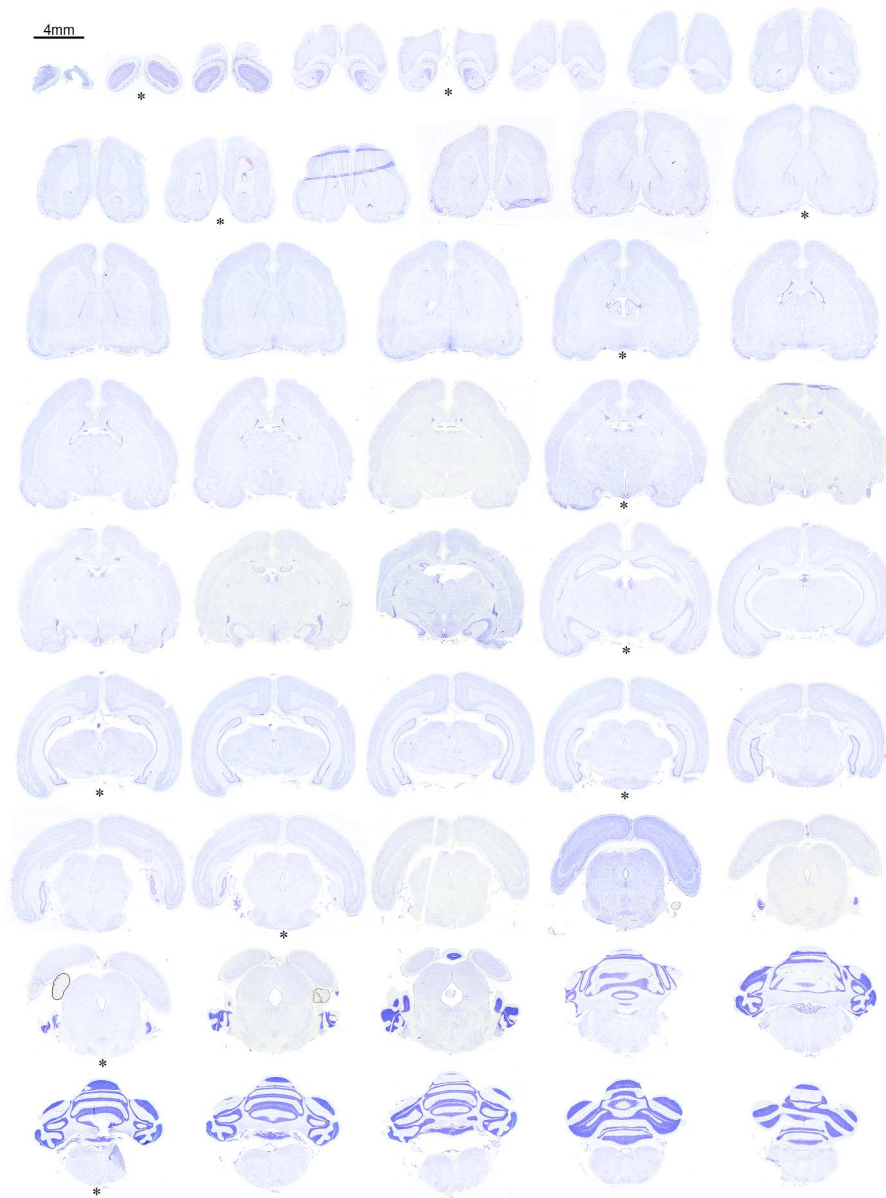


Figure 1. Histological sections displaying the cytoarchitecture of the *P. discolor* bat brain.

222x298mm (300 x 300 DPI)

AC



Figure 2. Histological sections displaying the cytoarchitecture of the *R. aegyptiacus* bat brain.

181x376mm (300 x 300 DPI)

AC

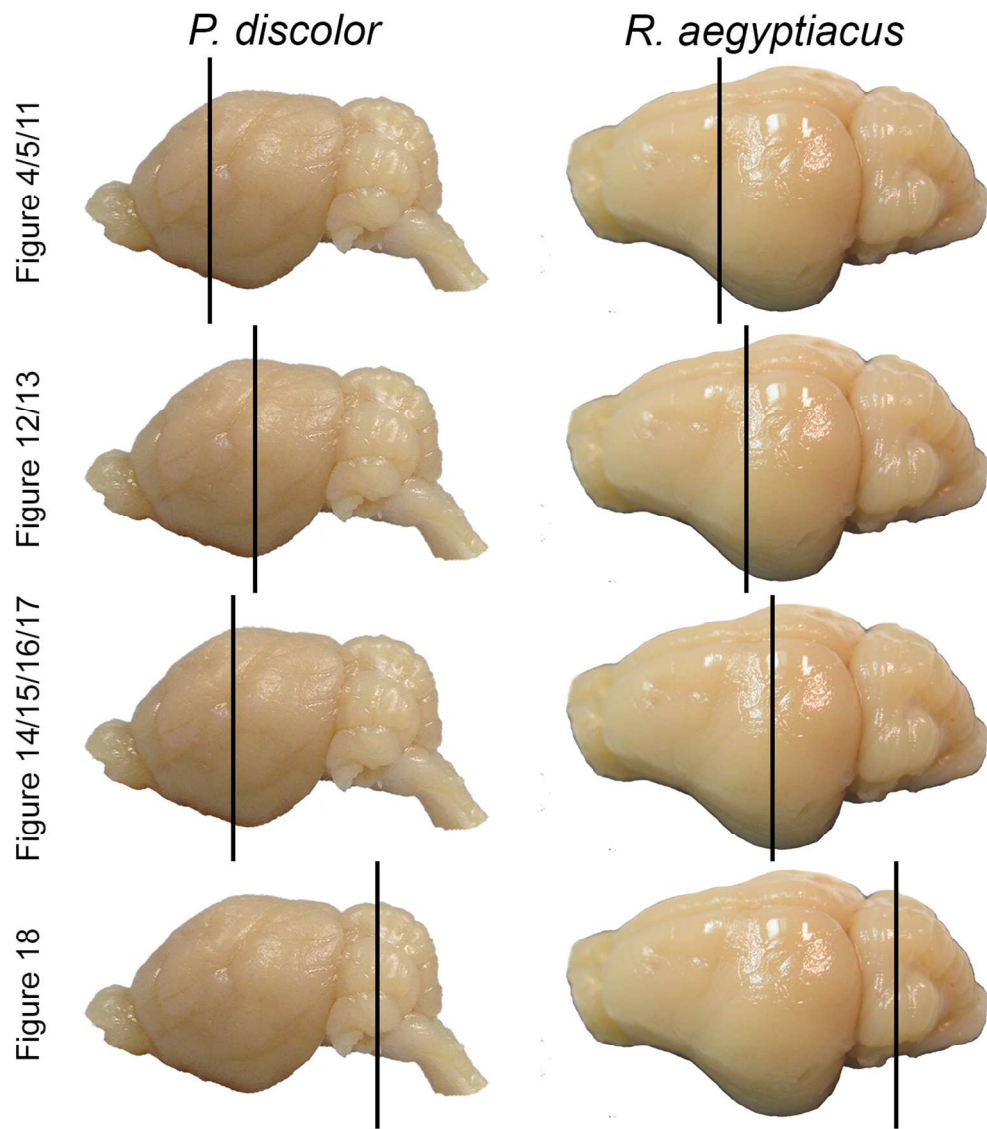


Figure 3. Whole dissected bat brains indicating depths of slices used for representative images.

119x139mm (300 x 300 DPI)

AC

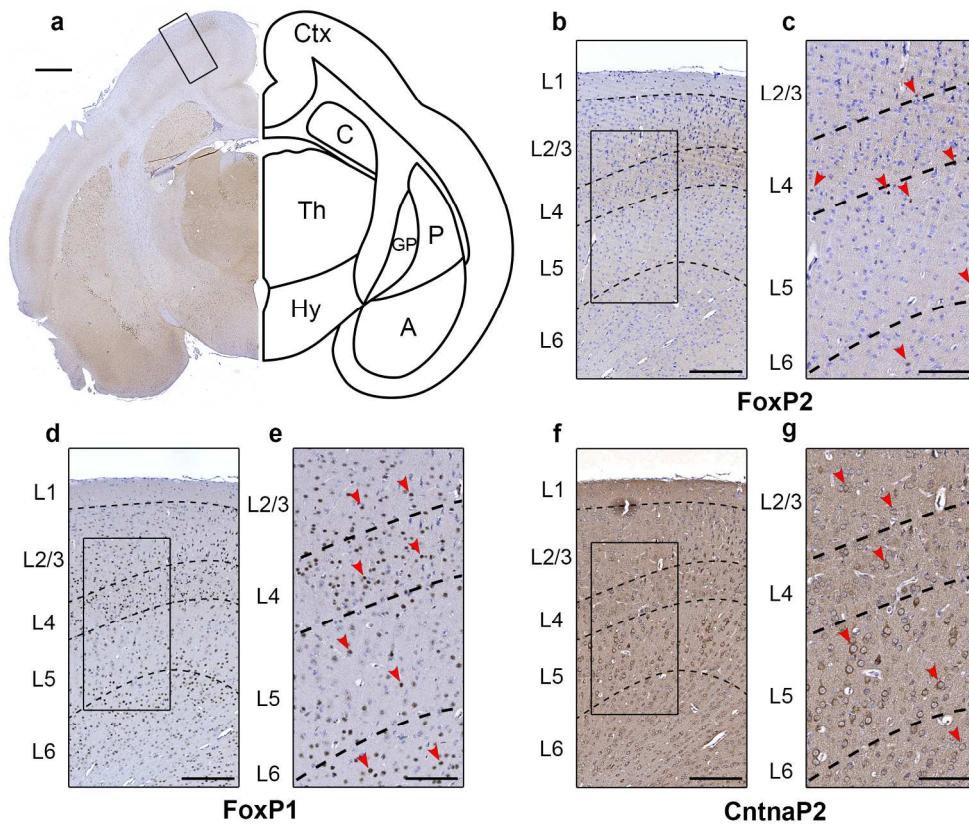


Figure 4. Examination of the P. discolor cortex reveals layer and species specific expression patterns.

195x163mm (300 x 300 DPI)

Accep

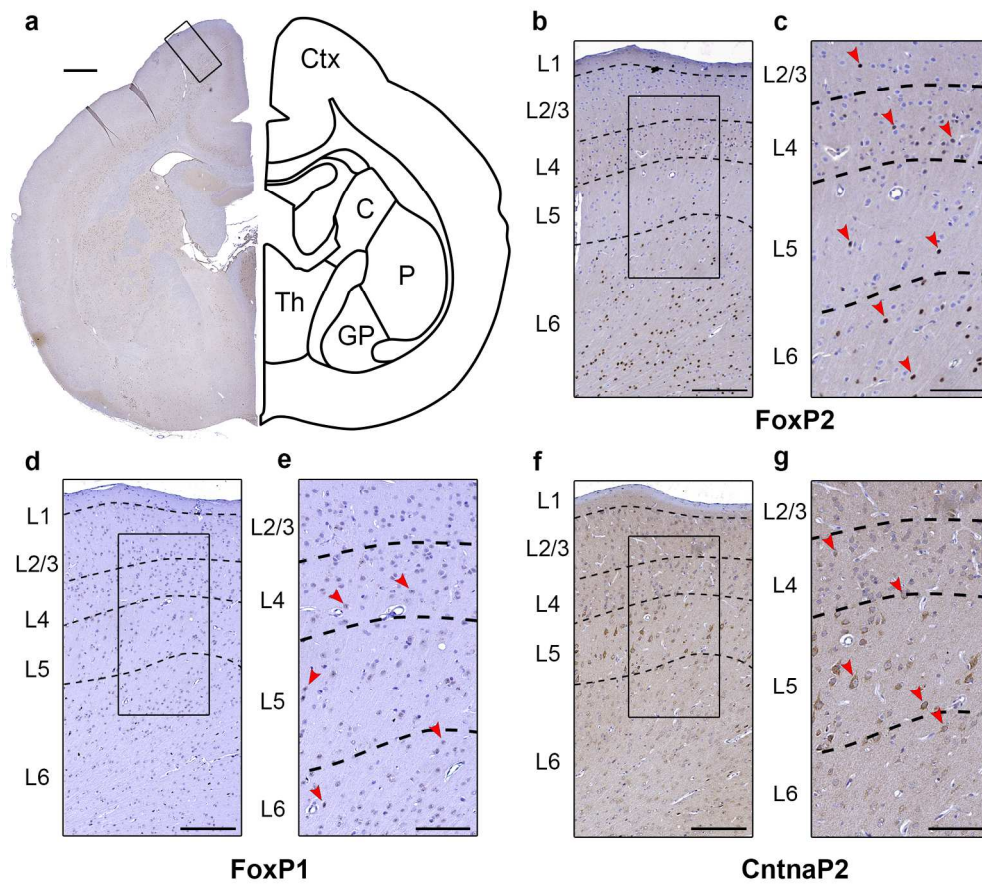


Figure 5. Examination of the *R. aegyptiacus* cortex reveals layer and species specific expression patterns.

186x167mm (300 x 300 DPI)

AcceJ

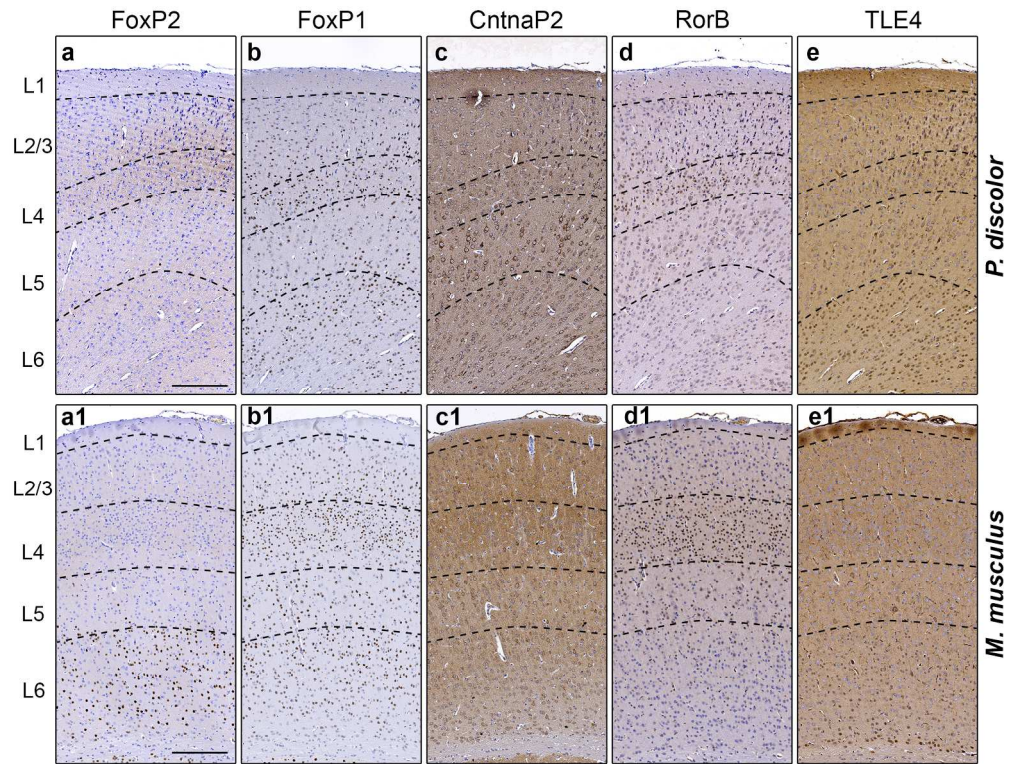
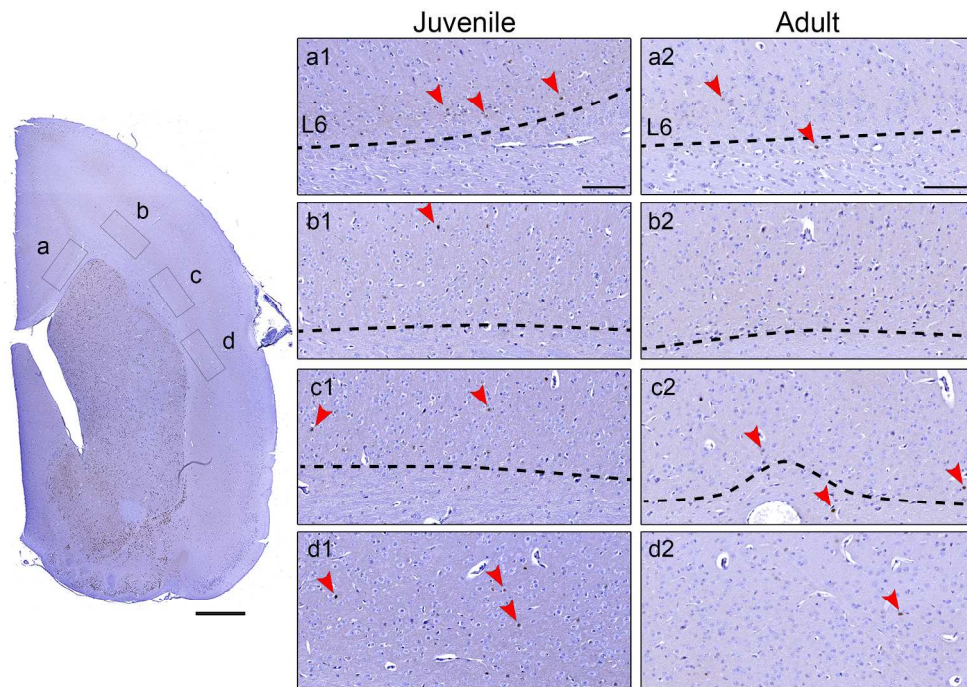


Figure 6. Cortical layering is conserved between mouse brains and *P. discolor* bats.

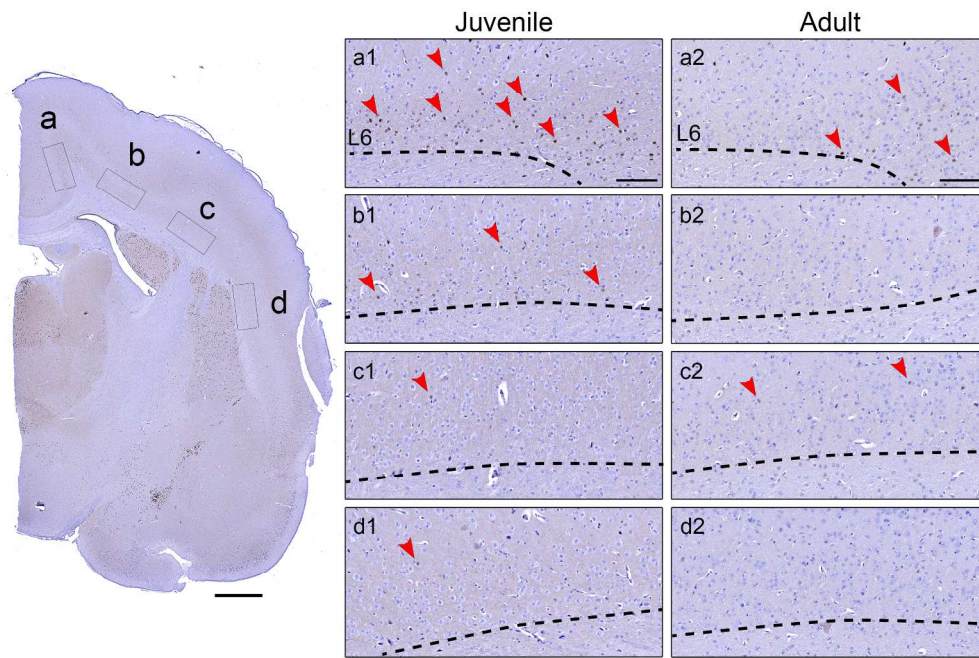
203x157mm (300 x 300 DPI)

Accepted



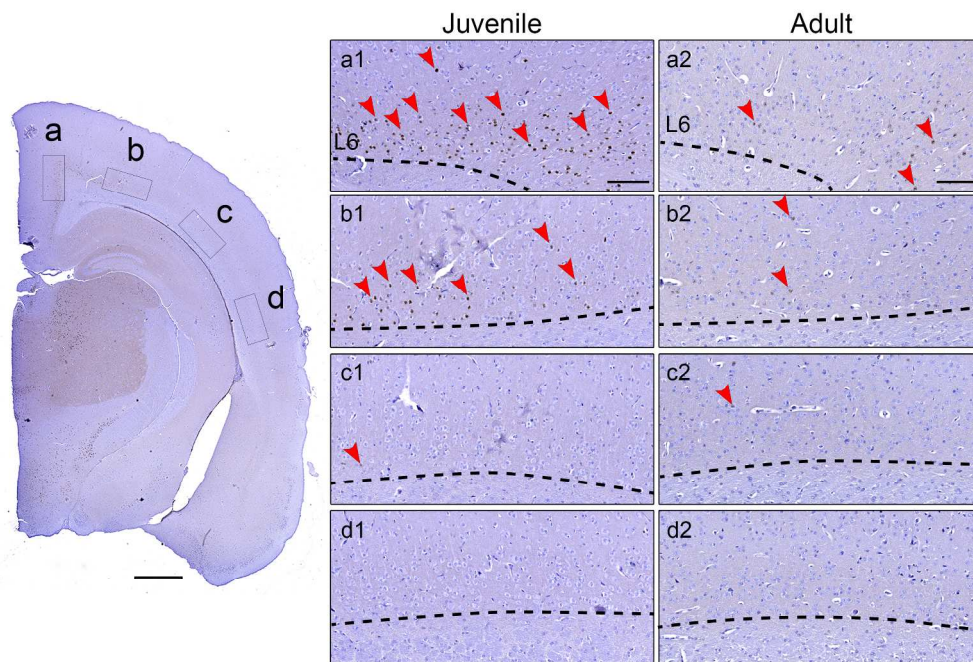
226x157mm (300 x 300 DPI)

Accepted



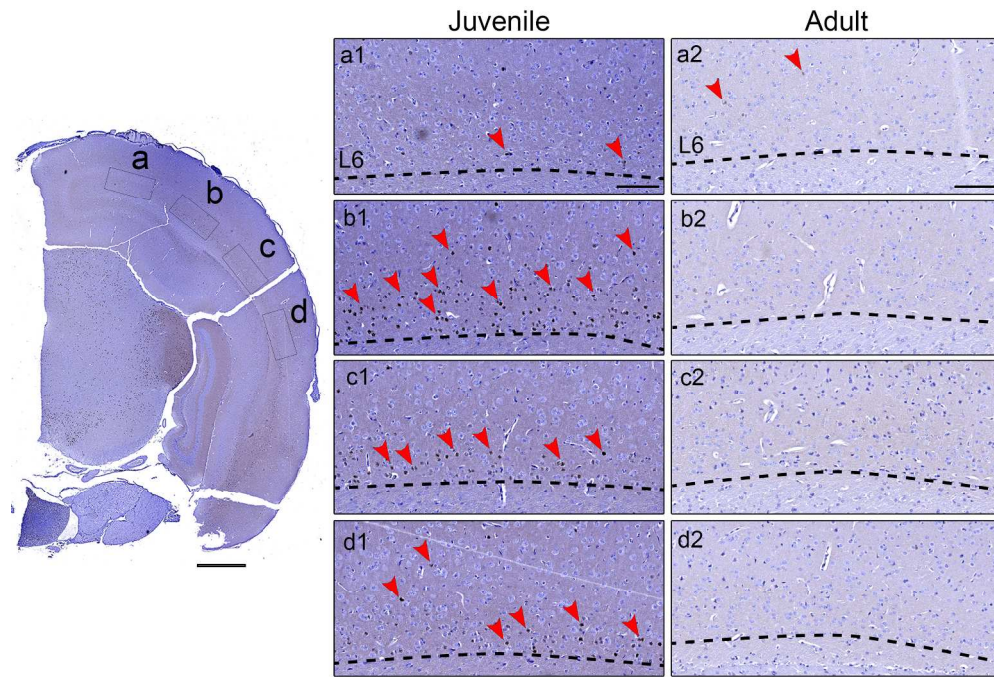
237x159mm (300 x 300 DPI)

Accepte



233x157mm (300 x 300 DPI)

Accept



228x156mm (300 x 300 DPI)

Accepted

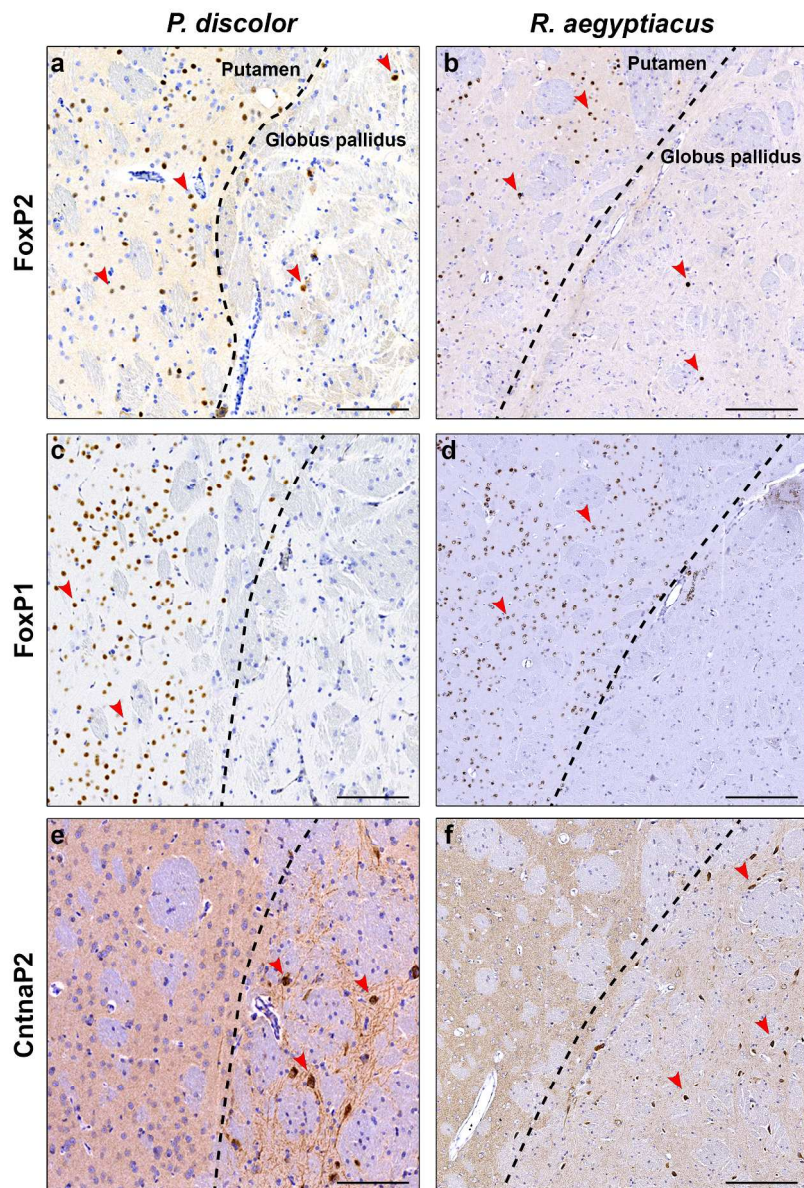


Figure 11. FoxP genes show an inverse expression pattern to CntnaP2 in compartments of the striatum of both bat species.

200x290mm (300 x 300 DPI)

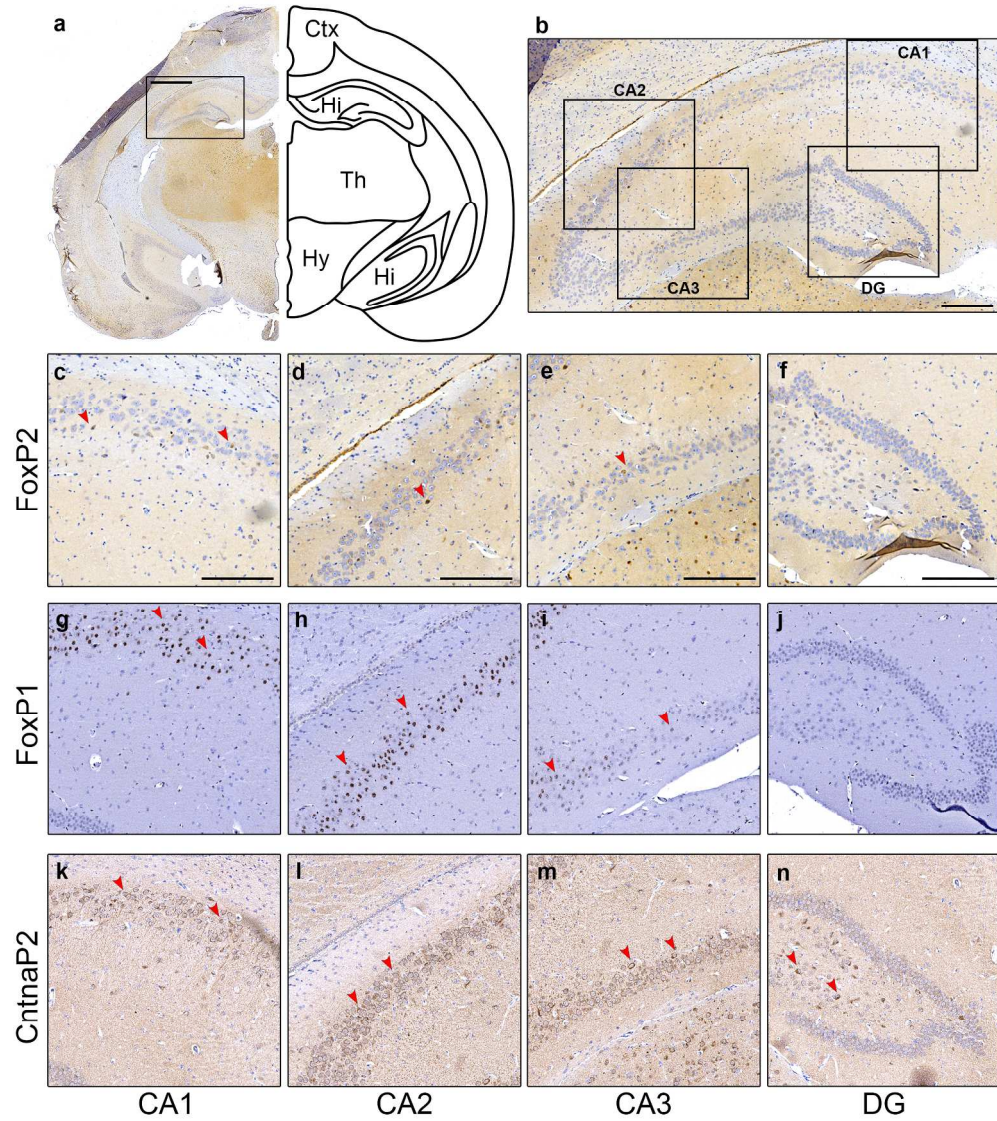


Figure 12. Distribution of FoxP2, FoxP1 and CntnaP2 in the hippocampus of *P. discolor*.

216x242mm (300 x 300 DPI)

Acc

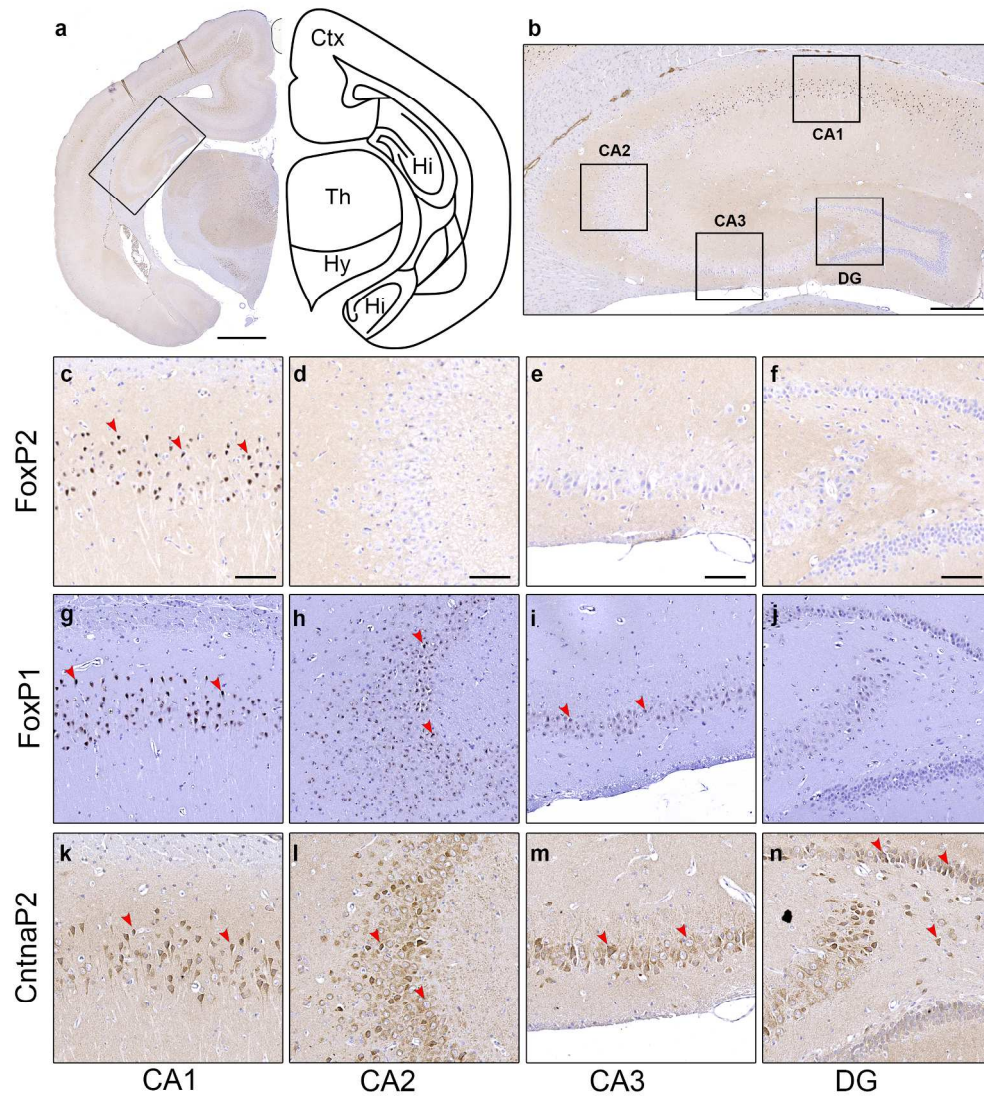


Figure 13. Distribution of FoxP2, FoxP1 and CntnaP2 in the hippocampus of *R. aegyptiacus*.

219x241mm (300 x 300 DPI)

Acc

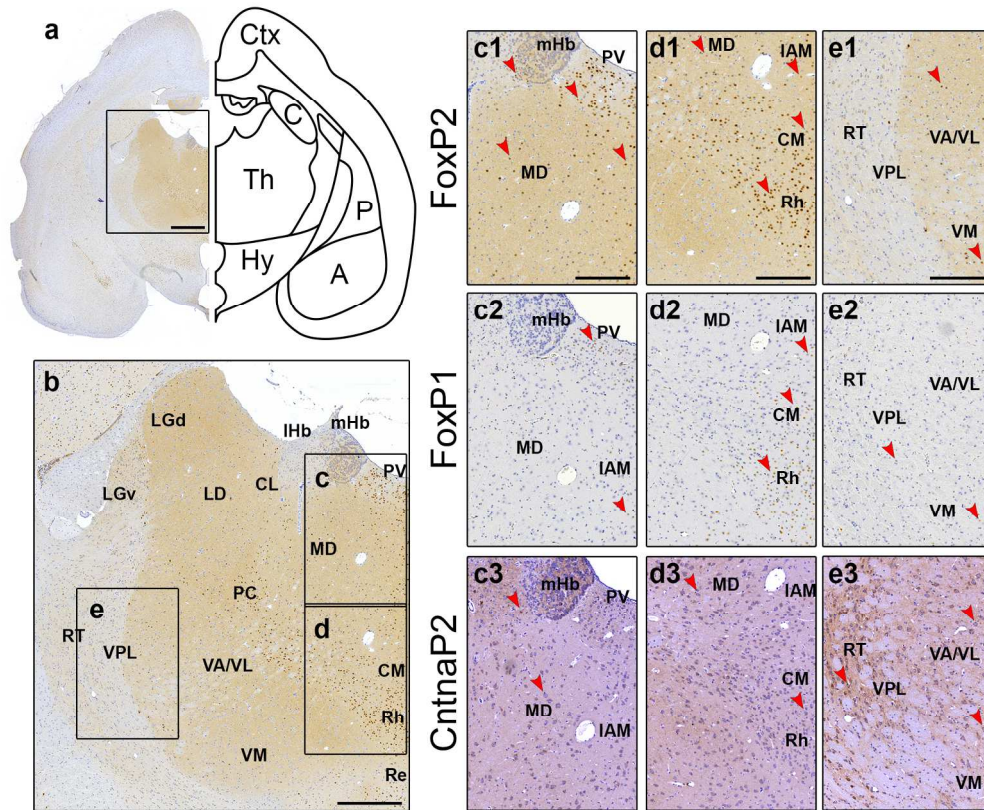


Figure 14. Distribution of FoxP2, FoxP1 and CntnaP2 in the thalamus of *P. discolor*.

178x146mm (300 x 300 DPI)

Accep

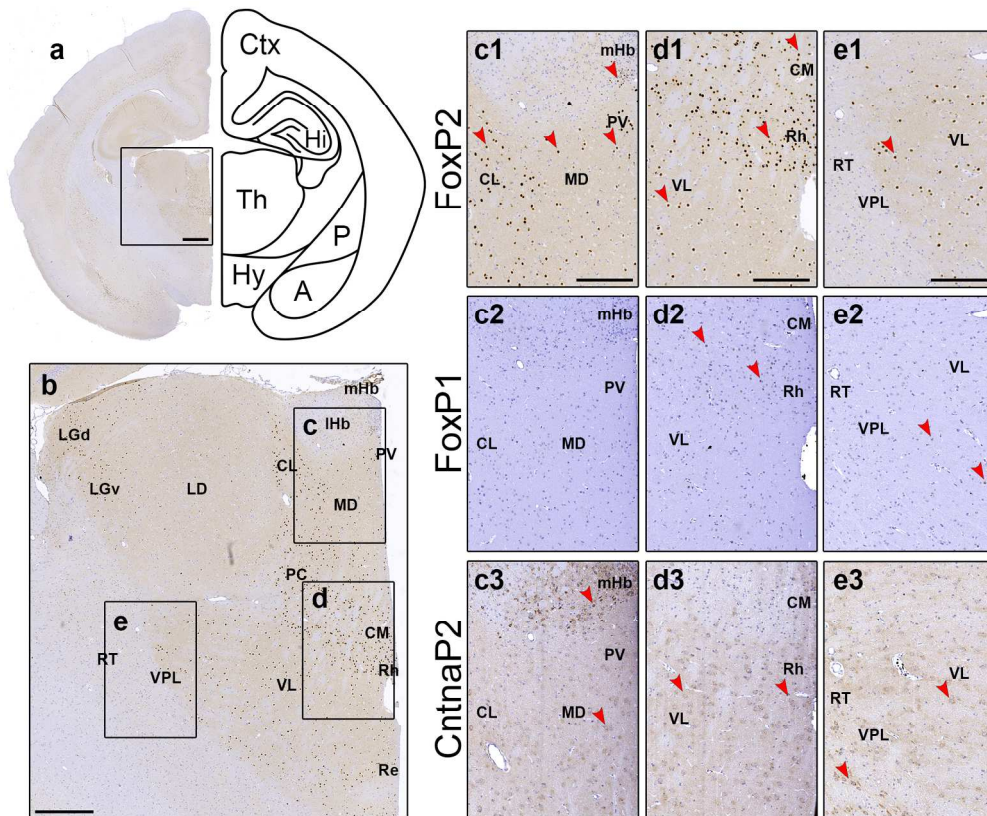


Figure 15. Distribution of FoxP2, FoxP1 and CntnaP2 in the thalamus of *R. aegyptiacus*.

177x145mm (300 x 300 DPI)

Accep

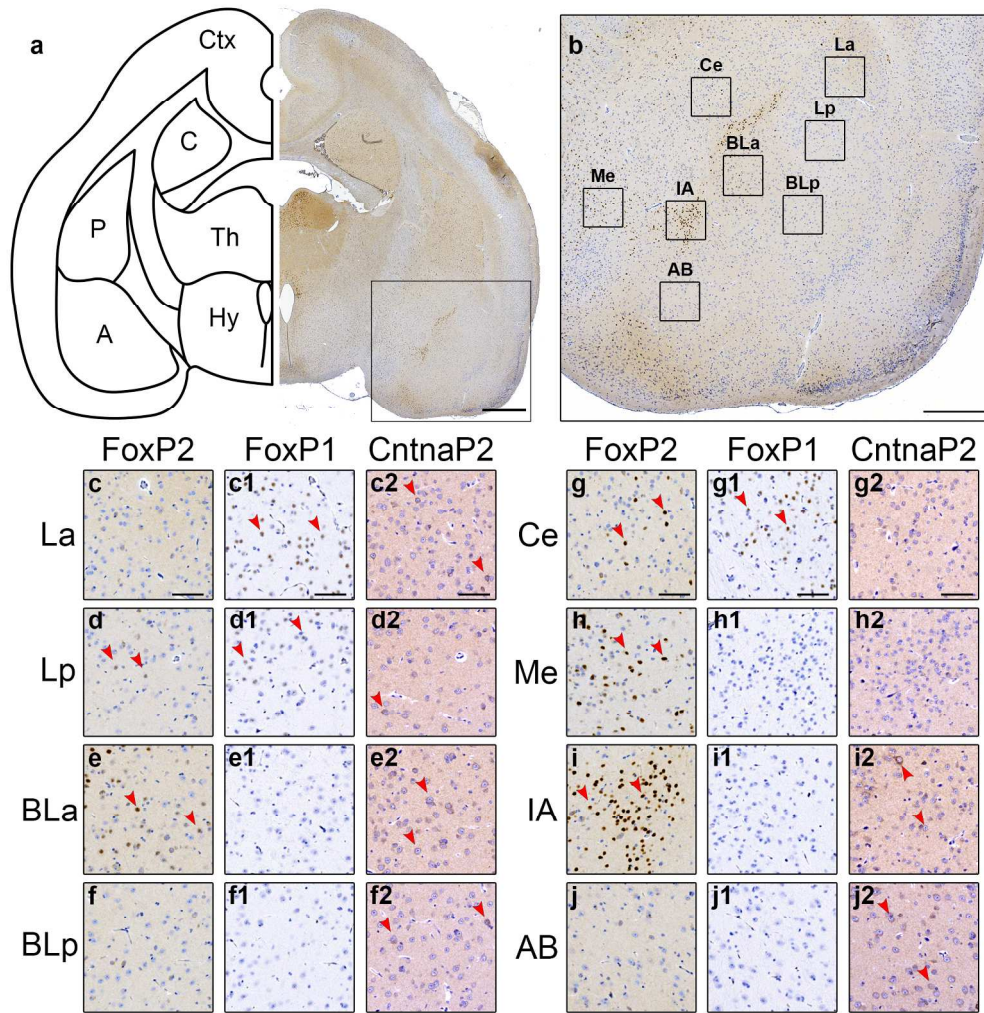


Figure 16. Distribution of FoxP2, FoxP1 and CntnaP2 in the amygdala of *P. discolor*.

195x199mm (300 x 300 DPI)

Acc

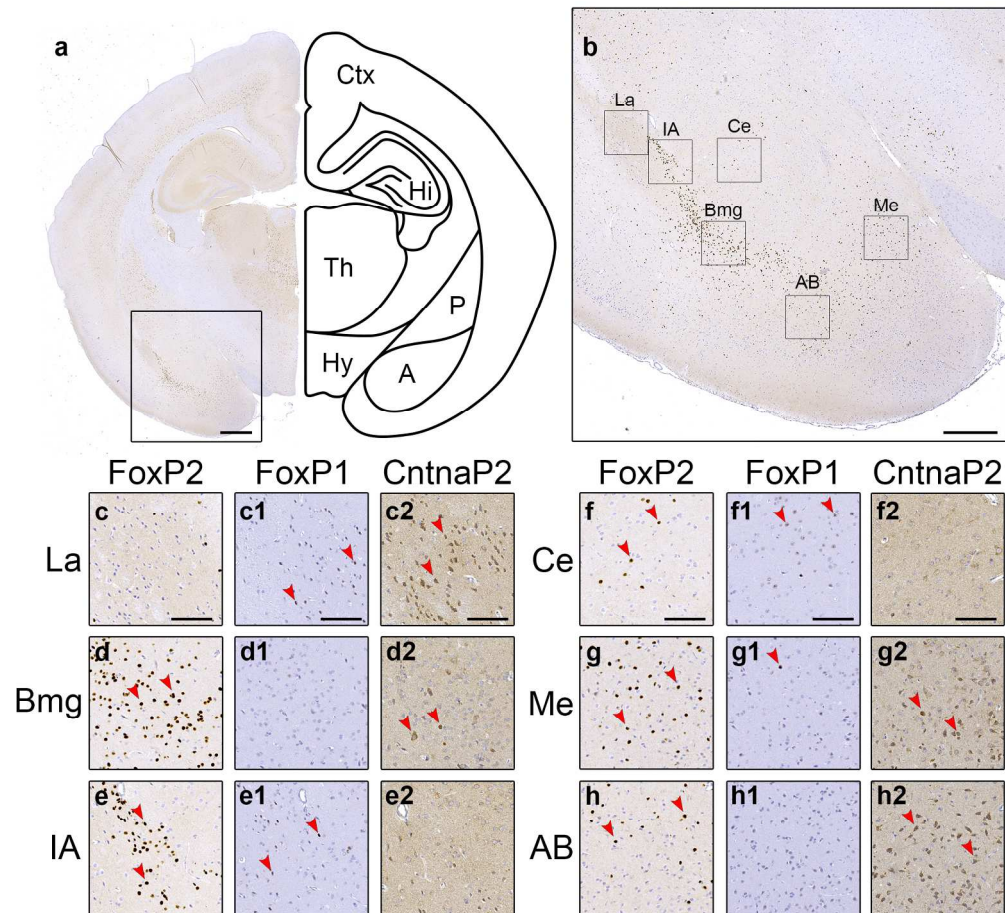


Figure 17. Distribution of FoxP2, FoxP1 and CntnaP2 in the amygdala of *R. aegyptiacus*

189x175mm (300 x 300 DPI)

Acce]

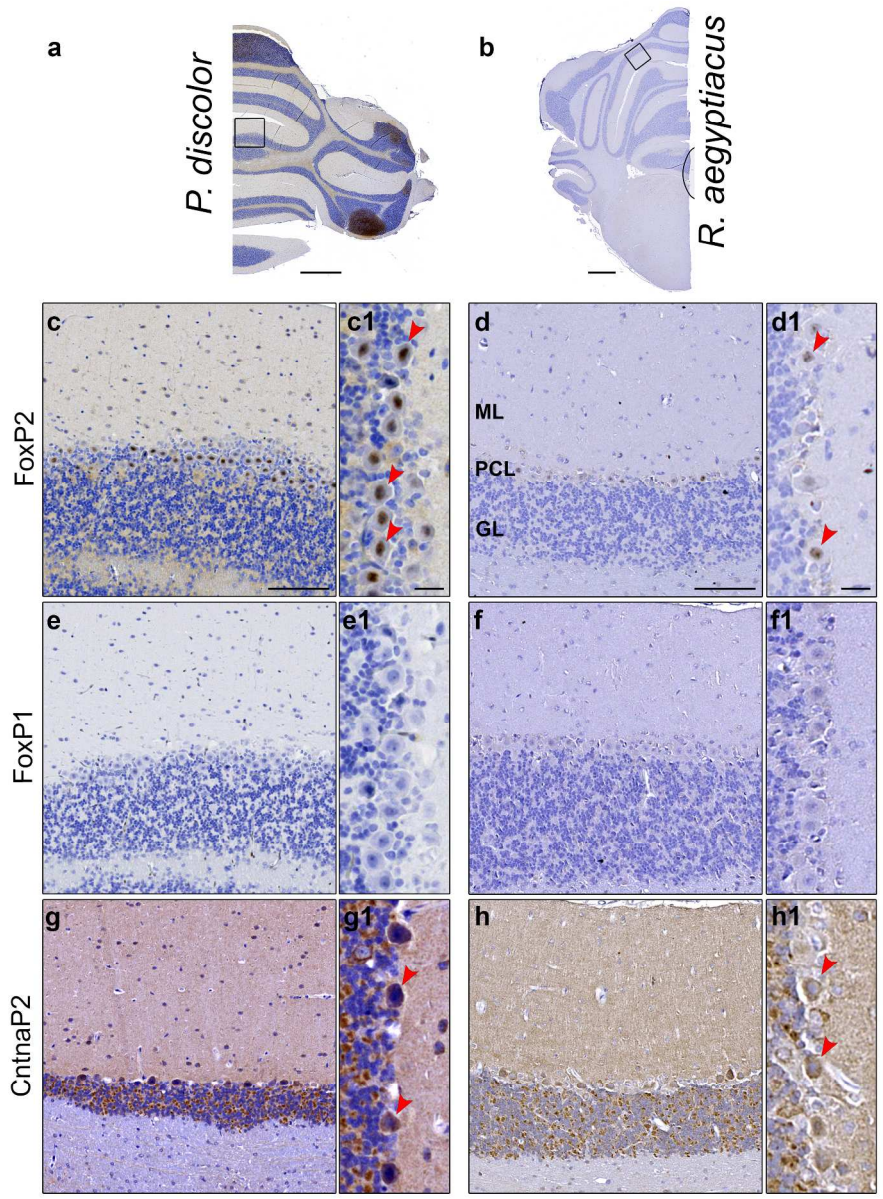


Figure 18

214x287mm (300 x 300 DPI)

AC

Name	Product #	Lot #	Company	Raised in	Antigen retrieval (pH)	Species used for	Primary antibody concentration	Block	Secondary antibody	Secondary product #	Company	Secondary concentration	Method
Foxp2 Banham	-	-	-	mouse	9	All species	1:250	10% normal goat serum	Poly-HRP-GAM/R/R	VWRKDPVO55HRP	Immunologic	1:2	Direct
RORB origene	TA806996	W001	Origene		9		1:100						
CNTNAP2 Novus	NBP1-49575	1012	Novus biological		6		1:200						
Foxp1 UMAB89	UM800020	W001	Origene		9	R. aegyptiacus	1:100		Biotinylated Goat anti-mouse	BA-9200	Vector Labs	1:1000	ABC
Foxp1 ab134055	ab134055	GR97096-11	Abcam	rabbit	9	P. discolor	1:100	10% normal horse serum	Biotinylated Horse anti-rabbit	BA-1100			
TLE4 origene	TA330275	-	Origene		9	All species	1:100						

Table 2. Comprehensive description of gene expression patterns in *P. discolor*

		FoxP2		FoxP1		CntnaP2		
		Intensity	Abundance	Intensity	Abundance	Intensity	Abundance	
Cerebral cortex	Isocortex							
	Cortex - layer I	-	-	-	-	-	-	
	Cortex - layer II/III	+++	Rare	++++	Medium	+	Rare	
	Cortex - layer IV	+++	Medium	++++	Abundant	+++	Rare	
	Cortex - layer V	+++	Rare	++	Abundant	+++++	Abundant	
	Cortex - layer VI	+	Rare	+++	Abundant	+	Medium	
		Olfactory areas						
		Olfactory bulb, glomerular layer	+++++	Abundant	++	Rare	-	-
		Olfactory bulb, outer plexiform layer	++++	Rare	+	Rare	+++	Rare
		Olfactory bulb, mitral cell layer	++	Medium	+++	Medium	++++	Abundant
		Olfactory bulb, inner plexiform layer	+++	Rare	+++	Rare	+++	Rare
		Olfactory bulb, granule layer	++++	Rare	+	Rare	+++	Rare
		Anterior olfactory nucleus, external layer	+++	Rare	-	-	++++	Abundant
		Lateral olfactory tract	++++	Rare	-	-	-	-
		Nucleus of the lateral olfactory tract	-	-	-	-	++++	Medium
		Cortical sub-plate						
		Clastrum	-	-	-	-	+	Abundant
		Endopyriform nucleus	-	-	-	-	+	Abundant
		Posterior pyriform area	-	-	-	-	+++	Rare
		Lateral amygdaloid nucleus, pars anterior	-	-	++	Abundant	+	Medium
		Lateral amygdaloid nucleus, pars posterior	-	-	+++	Abundant	-	-
		Basolateral amygdaloid nucleus, anterior	+++	Abundant	+	Medium	+	Abundant
		Basolateral amygdaloid nucleus, posterior	-	-	+	Abundant	-	-
		Accessory basal amygdaloid complex	-	-	+	Rare	-	-
		Anterior amygdaloid area	+++++	Abundant	+++	Medium	+++	Rare
		Posterolateral cortical amygdaloid nucleus	-	-	-	-	+	Rare
		Hippocampal formation						
		CA1	++	Rare	+++	Abundant	+++	Abundant
		CA2	+	Rare	+++	Abundant	+++	Abundant
		CA3	+	Rare	+	Medium	+++	Abundant
		Dentate gyrus, polymorph layer	-	-	-	-	+++	Rare
		Dentate gyrus, granule layer	-	-	-	-	-	-
	Subiculum	-	-	+++++	Abundant	+++	Rare	
Striatum	Dorsal region							
	Caudate nucleus	++++	Abundant	+++++	Abundant	++	Rare	
	Putamen	++++	Abundant	+++++	Abundant	++++	Rare	
		Ventral region						
	Nucleus accumbens	++++	Abundant	+++++	Abundant	+++	Rare	
	Olfactory tubercle	++++	Abundant	+++++	Abundant	+++++	Medium	
		Lateral septus						
	Lateral septal nucleus	++++	Abundant	+++	Medium	+	Rare	
		Striatum-like Amygdala						
	Medial amygdaloid nucleus	++++	Abundant	-	-	++	Medium	
	Central amygdaloid nucleus	+++	Rare	++	Abundant	-	-	
	Intercalated amygdaloid nucleus	+++++	Abundant	-	-	-	-	
		Pallidum						
	Globus pallidus	++++	Rare	-	-	+++++	Medium	
	Ventral pallidum	+++++	Abundant	-	-	-	-	
Substantia innominata	+++	Rare	-	-	+++	Abundant		
Medial septal nucleus	-	-	-	-	+++++	Abundant		
Diagonal band	-	-	+	Rare	+++++	Abundant		
Nucleus of the stria terminalis	++++	Rare	-	-	++	Rare		
	Anterior group							
Anteroventral nucleus	-	-	-	-	++++	Abundant		

Thalamus	Anteromedial nucleus	-	-	-	-	++	Abundant	
	Interanterodorsal nucleus	-	-	-	-	+++	Abundant	
	Interanteromedial nucleus	+++	Medium	+	Medium	++	Abundant	
	Laterodorsal nucleus	+	Rare	-	-	++++	Abundant	
	Lateral group							
	Lateral posterior nucleus	+++	Abundant	-	-	+++	Abundant	
	Posterior thalamic nucleus	+++	Abundant	+++	Medium	++	Abundant	
	Suprageniculate nucleus	+++++	Abundant	-	-	+++	Abundant	
	Medial group							
	Intermediodorsal nucleus	+++++	Abundant	+	Abundant	++	Abundant	
	Mediodorsal thalamus	+	Abundant	-	-	+++	Abundant	
	submedial nucleus of the thalamus	-	-	+++++	Medium	+++	Medium	
	Midline group							
	Paraventricular nucleus	+++++	Abundant	+++	Abundant	+++	Abundant	
	Paratenial nucleus	+++	Medium	-	-	+++	Abundant	
	Nucleus reuniens*	+++	Medium	+++	Medium	+	Abundant	
	Ventral nuclear group							
	Ventro anterior nucleus	-	-	+	Medium	+++	Abundant	
	Ventrolateral nucleus	+++	Abundant	+	Medium	+++	Abundant	
	Ventromedial nucleus	+++	Rare	+++	Rare	++	Abundant	
	Ventroposteromedial nucleus	+++	Abundant	-	-	++++	Abundant	
	Ventroposterolateral nucleus	+++	Abundant	+++	Rare	++++	Abundant	
	Intralaminar nuclei							
	Rhomboidal nucleus	+++++	Abundant	+++	Abundant	+	Abundant	
	Centromedial nucleus	+++++	Abundant	+++	Medium	++	Abundant	
	Paracentral nucleus	+++++	Abundant	-	-	++	Abundant	
	Centrolateral nucleus	+++++	Abundant	-	-	+	Abundant	
	Parafascicular nucleus	+++++	Abundant	+++++	Abundant	-	-	
	Geniculate group							
	Lateral geniculate nucleus, dorsal	+++++	Medium	++	Rare	+++++	Abundant	
Lateral geniculate nucleus, ventral	+++++	Rare	+++	Medium	+++	Rare		
Medial geniculate nucleus, dorsal	+++	Abundant	-	-	+++	Abundant		
Medial geniculate nucleus, ventral	+++	Abundant	-	-	+++	Abundant		
Medial geniculate nucleus, magnocellular	+++++	Abundant	-	-	+++	Abundant		
Other								
Reticular nucleus of the thalamus	-	-	-	-	++++	Abundant		
Subparafascicular nucleus	+++++	Abundant	+++++	Abundant	-	-		
Epithalamus								
Habenular nucleus, medial	+++	Rare	-	-	++++	Medium		
Habenular nucleus, lateral	++	Rare	-	-	+++++	Medium		
Hypothalamus								
Periventricular								
Paraventricular nucleus of hypothalamus	+++++	Abundant	++++	Medium	+++++	Abundant		
Supraoptic nucleus	++++	Medium	+++++	Abundant	++++	Abundant		
Arcuate	+++++	Medium	+	Medium	-	-		
Dorsomedial hypothalamic nucleus	++++	Abundant	-	-	++	Medium		
Median preoptic nucleus	+	Medium	++++	Rare	-	-		
Medial								
Medial preoptic area	-	-	++++	Rare	+++	Abundant		
Anterior hypothalamic nucleus	+++++	Abundant	-	-	-	-		
Posterior hypothalamic nucleus	+++++	Medium	-	-	+	Medium		
Lateral								
Lateral hypothalamic area	++	Medium	++	Medium	+	Medium		
Lateral preoptic area	+++++	Abundant	+++	Medium	+	Medium		
Subthalamic nucleus	+++++	Abundant	+++	Rare	+++	Abundant		
Zona incerta, subthalamus	-	-	+++	Rare	++	Abundant		
Tuberal nucleus	++	Abundant	+	Abundant	-	-		
Sensory related								
Superior colliculus, superficial gray layer // optic layer	+++++	Medium	++	Rare	+++	Medium		

	Inferior colliculus, external nucleus	++++	Rare	+++	Rare	+++	Rare	
	Inferior colliculus	+++++	Abundant	+	Rare	++++	Abundant	
	Parabigeminal nucleus	+++++	Abundant	-	-	-	-	
	Motor related							
Midbrain	Oculomotor nucleus	+++++	Rare	-	-	+++++	Abundant	
	Midbrain reticular nucleus	+++++	Medium	++	Rare	++++	Abundant	
	Superior colliculus, motor related	++++	Medium	++	Rare	++++	Abundant	
	Ventral tegmental area	+++	Abundant	-	-	+++++	Abundant	
	Periaqueductal gray	+++	Medium	+	Rare	++++	Medium	
	Interstitial nucleus of Cajal	+++++	Medium	-	-	+++++	Medium	
	Nucleus of Darkschewitsch	+++++	Abundant	-	-	+++++	Abundant	
	Substantia nigra, reticular part	+++++	Medium	+++++	Medium	+++++	Abundant	
	Anterior pretectal nucleus	++++	Abundant	++	Rare	++++	Abundant	
	Nucleus of the posterior commissure	+++++	Medium	+	Rare	++++	Medium	
	Olivary pretectal nucleus	++++	Medium	+	Medium	+++++	Medium	
	Posterior pretectal nucleus	-	-	++	Rare	+++	Rare	
	Red nucleus	-	-	-	-	+++	Abundant	
		Behavioural state related						
		Substantia nigra, compact part	+++	Abundant	+	Rare	++++	Abundant
	Interfascicular nucleus Raphe	+++++	Abundant	+++	Medium	-	-	
	Interpeduncular nucleus	-	-	-	-	+++	Medium	
	Rostral linear Raphe nucleus	+++	Rare	-	-	-	-	
	Central linear Raphe nucleus	++++	Rare	-	-	+++	Abundant	
	Dorsal Raphe nucleus	+++++	Medium	+	Rare	+++++	Abundant	
	Pons sensory related							
Hindbrain	Nucleus of the lateral lemniscus, dorsal and horizontal part	+++++	Abundant	-	-	-	-	
	Nucleus of the lateral lemniscus, ventral part	+++	Abundant	+++	Abundant	+++++	Abundant	
	Periolivary complex	-	-	-	-	+++	Medium	
		Pons motor related						
	Pontine reticular formation	++++	Rare	-	-	++++	Medium	
	Pontine gray	-	-	-	-	+++++	Abundant	
	Dorsal tegmental nucleus	+++	Medium	-	-	++++	Medium	
	Tegmental reticular nucleus	-	-	-	-	+++++	Abundant	
		Pons behavioural state related						
		Superior central nucleus Raphe, medial part	+	Medium	+++	Rare	+++++	Abundant
	Superior central nucleus Raphe, lateral part	+++	Rare	-	-	++++	Medium	
	Pontine reticular nucleus	+++++	Rare	+++	Rare	+++	Abundant	
	Cortex							
Cerebellum	Molecular layer	-	-	-	-	-	-	
	Purkinje cells	++++	Abundant	-	-	+	Medium	
	Granular layer	-	-	-	-	+++++	Abundant	

Table 3. Comprehensive description of gene expression patterns in *R. aegyptiacus*

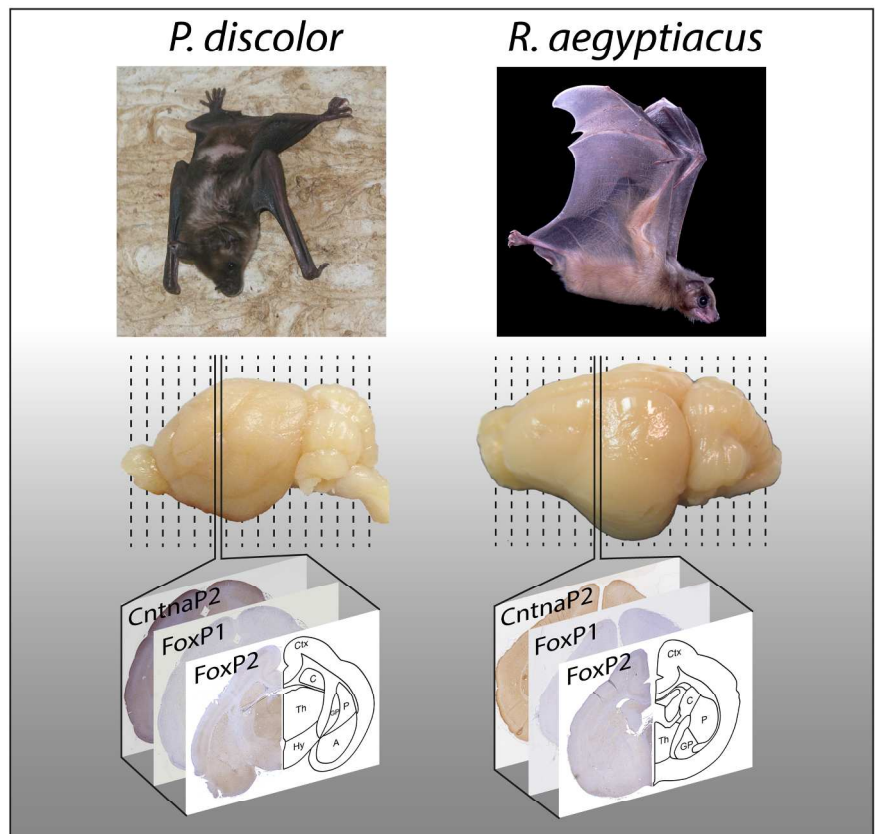
	FoxP2		FoxP1		CntnaP2		
	Intensity	Abundance	Intensity	Abundance	Intensity	Abundance	
Cerebral cortex	Isocortex						
	Cortex - layer I	-	-	-	-	-	-
	Cortex - layer II/III	-	-	++	Abundant	+	Abundant
	Cortex - layer IV	+	Abundant	++	Abundant	-	-
	Cortex - layer V	+++	Rare	++	Abundant	+++++	Abundant
	Cortex - layer VI	++++	Abundant	++	Abundant	+	Abundant
	Olfactory areas						
	Olfactory bulb, glomerular layer	+++++	Abundant	-	-	+	Rare
	Olfactory bulb, outer plexiform layer	+	Rare	-	-	+	Abundant
	Olfactory bulb, mitral cell layer	-	-	-	-	+++++	Abundant
	Olfactory bulb, inner plexiform layer	+++++	Rare	-	-	-	-
	Olfactory bulb, granule layer	+++++	Rare	-	-	+++	Rare
	Anterior olfactory nucleus	+++	Rare	++	Abundant	++	Abundant
	Anterior olfactory nucleus, medial	+++	Medium	++	Abundant	++	Abundant
	Anterior olfactory nucleus, dorsal	+++	Medium	++	Abundant	+	Abundant
	Anterior olfactory nucleus, lateral	-	-	++	Abundant	++++	Abundant
	Anterior olfactory nucleus, posteroventral	+++++	Rare	++	Abundant	++++	Abundant
	Anterior olfactory nucleus, external part	-	-	-	-	+++++	Abundant
	Nucleus of the lateral olfactory tract	-	-	-	-	+++	Abundant
	Cortical amygdalar area	+++	Medium	-	-	++++	Abundant
Cortical sub-plate							
Clastrum	-	-	-	-	+++	Medium	
Pyramidal area, layer 2	-	-	-	-	+++++	Abundant	
Posterior pyramidal area	-	-	-	-	-	-	
Lateral amygdaloid nucleus	-	-	+++++	Abundant	+++	Abundant	
Accessory basal amygdaloid complex	+++	Medium	-	-	+++	Abundant	
Anterior amygdaloid area	+++++	Medium	-	-	+++	Rare	
Hippocampal formation							
CA1	+++	Abundant	+++++	Abundant	++++	Abundant	
CA2	-	-	+++	Abundant	++++	Abundant	
CA3	-	-	+	Abundant	++++	Abundant	
Dentate gyrus, polymorph layer	-	-	-	-	+++	Medium	
Dentate gyrus, granule layer	-	-	-	-	+	Rare	
Subiculum	++++	Abundant	+++	Abundant	-	-	
Striatum	Dorsal region						
	Caudate nucleus	++++	Abundant	+++++	Abundant	+	Rare
	Putamen	++++	Abundant	+++++	Abundant	+	Rare
	Ventral region						
	Nucleus accumbens	++++	Abundant	+++++	Abundant	+	Rare
	Olfactory tubercle	+++++	Abundant	++++	Abundant	+++	Medium
	Striatum-like Amygdala						
	Medial amygdaloid nucleus	++++	Abundant	+++	Rare	+++	Abundant
	Central amygdaloid nucleus	+++	Rare	+++	Medium	+++	Rare
	Intercalated amygdalar nucleus	+++++	Abundant	-	-	-	-
	Basal magnocellular nucleus	+++++	Abundant	-	-	-	-
	Pallidum						
	Globus pallidus	+++++	Rare	-	-	+++++	Medium
Diagonal band	+++	Rare	-	-	+++++	Abundant	
Nuclear of the stria terminalis	++++	Medium	-	-	-	-	
Anterior group	Anterior group						
	Anteromedial nucleus	-	-	-	-	+++	Abundant
	Anteromedial nucleus	-	-	-	-	+	Abundant
	Laterodorsal nucleus	-	-	-	-	-	-
	Lateral group						
	Lateral posterior nucleus	+++	Abundant	-	-	+	Abundant
	Posterior thalamic nucleus	+++	Abundant	+++	Abundant	+	Abundant
Medial group							

Thalamus	Mediodorsal thalamus	+++	Abundant	-	-	+	Rare
	Midline group						
	Paraventricular nucleus	+++++	Abundant	-	-	+	Abundant
	Nucleus reuniens*	+++++	Abundant	-	-	+++	Medium
	Ventral nuclear group						
	Ventro anterior nucleus	-	-	-	-	+	Abundant
	Ventrolateral nucleus	+++	Medium	-	-	+	Abundant
	Ventromedial nucleus	-	-	++++	Abundant	-	-
	Ventroposteromedial nucleus	++++	Abundant	++++	Abundant	+	Abundant
	Ventroposterolateral nucleus	-	-	++++	Abundant	+	Abundant
	Intralaminar nuclei						
	Rhomboidal nucleus	+++++	Abundant	++++	Abundant	+	Abundant
	Centromedial nucleus	+++++	Abundant	-	-	++	Abundant
	Paracentral nucleus	+++++	Abundant	-	-	++	Abundant
	Centrolateral nucleus	+++++	Abundant	-	-	+++	Abundant
	Parafascicular nucleus	+++++	Abundant	+++	Abundant	-	-
	Geniculate group						
	Lateral geniculate nucleus, dorsal	++	Abundant	++	Rare	-	-
	Lateral geniculate nucleus, ventral	+++	Rare	++	Rare	+++	Abundant
	Medial geniculate nucleus, dorsal	++++	Abundant	-	-	-	-
	Medial geniculate nucleus, ventral	++++	Abundant	-	-	-	-
Medial geniculate nucleus, magnocellular	+++	Abundant	-	-	-	-	
Other							
Reticular nucleus of the thalamus	-	-	-	-	+++	Abundant	
Epithalamus							
Habenular nucleus, medial	+++	Rare	-	-	+++++	Abundant	
Habenular nucleus, lateral	+++	Rare	-	-	+++++	Medium	
Hypothalamus	Periventricular						
	Paraventricular nucleus of hypothalamus	+++	Medium	+++	Rare	+++++	Medium
	Supraoptic nucleus	++++	Abundant	+++++	Medium	+++++	Abundant
	Dorsomedial hypothalamic nucleus	-	-	-	-	-	-
	Lateral preoptic area	+++++	Medium	-	-	+	Medium
	Medial						
	Medial preoptic area	+++++	Medium	-	-	+++++	Abundant
	Ventromedial hypothalamic nucleus	+++	Rare	-	-	+++++	Abundant
	Medial eminence	+++++	Rare	-	-	+++++	Abundant
	Lateral						
Lateral preoptic area	-	-	-	-	-	-	
Zona incerta, subthalamus	+++	Rare	-	-	-	-	
Midbrain	Sensory related						
	Superior colliculus, superficial gray layer // optic layer	++++	Abundant	++	Rare	++	Medium
	Motor related						
	Superior colliculus, motor related	++++	Abundant	++	Rare	++	Medium
	Ventral tegmental area	+++++	Abundant	++	Rare	+++	Medium
	Periaqueductal gray	+++	Medium	++	Rare	++++	Medium
	Substantia nigra, reticular part	+++	Medium	+++	Medium	+++	Abundant
	Anterior pretectal nucleus	+++	Medium	-	-	++	Medium
Behavioural state related							
Substantia nigra, compact part	+++++	Abundant	-	-	+++	Abundant	
Cerebellum	Cortex						
	Molecular layer	-	-	-	-	-	-
	Purkinje cells	++++	Abundant	-	-	++	Medium
Granular layer	-	-	-	-	+++++	Abundant	

We used immunohistochemistry to detail the expression of three language-related genes in the brains of two vocal learning bat species; *Phyllostomus discolor* and *Rousettus aegyptiacus*. We provide detailed distribution patterns of the FoxP2, FoxP1 and Cntnap2 proteins, accompanied by detailed cytoarchitectural histology across these bat brains. We created an online, open-access database (the BATLAS portal) within which all data can be browsed, searched, and high resolution images viewed to single cell resolution. The data presented herein reveal regions of interest in the bat brain and provide new opportunities to address the role of these language-related genes in complex vocal-motor and vocal learning behaviours in a mammalian model system.

Accepted Article

BATLAS: Bat Brain Atlas



207x199mm (300 x 300 DPI)

Acce